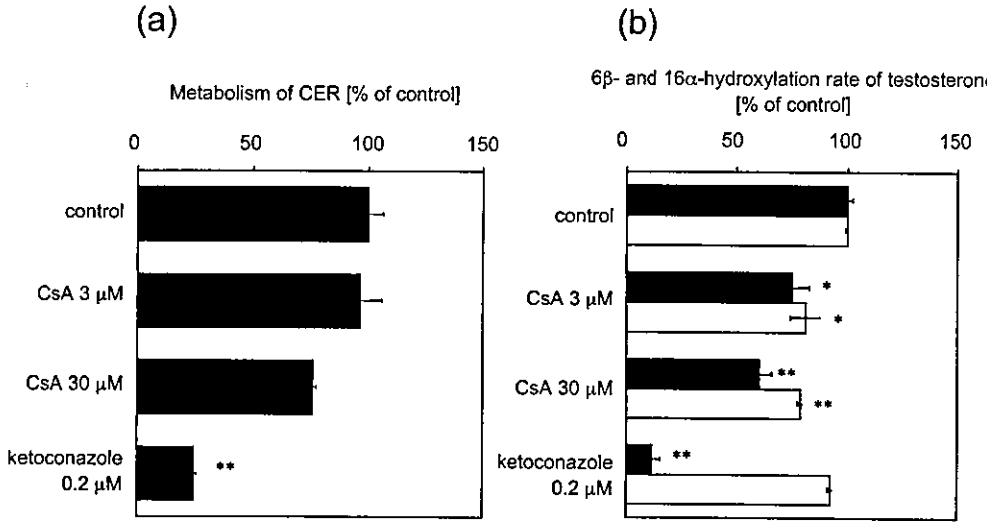

FIG. 6. Metabolic stability of CER and testosterone 6β- and 16α-hydroxylation in rat liver microsomes in the presence or absence of CsA or ketoconazole. In a, the effects of CsA and ketoconazole on the metabolism of CER in rat liver microsomes were examined. In b, those for testosterone 6β- (■) and 16α-hydroxylation (□) were examined. The metabolic rate in the presence or absence of inhibitors is shown in each figure. Each bar represents the mean ± S.E. (n = 3). The asterisk represents a statistically significant difference from control shown by Dunnett's test (*, $p < 0.05$; **, $p < 0.01$).

found that the Oatp1a1-mediated uptake of CER was inhibited by CsA in a concentration-dependent manner (Table 2), also supporting the involvement of Oatp transporter(s) in the hepatic uptake of CER.

We investigated the inhibitory effect of CsA on the uptake of CER in rat hepatocytes in the presence of 90% rat plasma, which was similar to in vivo conditions. In the presence of 90% rat plasma, the $IC_{50,app}$ value was approximately 12 times higher than the IC_{50} value in its absence (Fig. 2). Lemaire and Tillement (1982) reported that approximately 90% of CsA is bound to plasma proteins, mainly lipoprotein in rats. Taking this into consideration, the IC_{50} value, based on the estimated free concentration of CsA in the presence of 90% rat plasma, was calculated to be 0.232 μM, which is close to the IC_{50} value obtained in the study without rat plasma. The LUI study confirmed that the hepatic CER uptake measured in vivo was also affected by CsA (Fig. 5). When the blood concentration of CsA was 4 μM, the hepatic uptake of CER in the LUI study was reduced to 50% of the control value (Fig. 5), suggesting that the IC_{50} value for the in vivo hepatic uptake of CER was approximately 4 μM, which was similar to the $IC_{50,app}$ value estimated in the presence of plasma (Fig. 2b).

We have also examined the effect of CsA on the metabolism of CER in rat liver microsomes (Fig. 5). Only 26% of [^{14}C]CER was metabolized following a 2-h incubation in rat liver microsomes, whereas more than 50% was metabolized in human liver microsomes within 45 min (Shitara et al., 2003), suggesting slower metabolism in rat liver microsomes compared with their human counterparts. Since this metabolism of [^{14}C]CER was not significantly inhibited by CsA up to its concentration of 30 μM (Fig. 5), microsomal metabolism was not the mechanism for the pharmacokinetic interaction between CER and CsA in rats examined in the present study.

The results obtained in the in vitro studies should be quantitatively discussed in relation to those in vivo. Without administration of CsA, the CL_{tot} was estimated to be 1.51 l/h/kg (Table 1). In the case of CER, the urinary excretion is negligible (Boberg et al., 1998) and, therefore, the CL_{tot} is close to the hepatic clearance (CL_H). Assuming a well stirred model, the CL_H can be described by the following equation (Miyauchi et al., 1993; Yamazaki et al., 1996):

$$CL_H = \frac{Q_H \times f_b \times CL_{int,all}}{Q_H + f_b \times CL_{int,all}} \quad (5)$$

where Q_H is the hepatic blood flow and f_b is the blood unbound fraction. The $CL_{int,all}$ represents the overall intrinsic hepatic clearance, which includes membrane permeability, metabolism, and biliary excretion, as described by the following equation:

$$CL_{int,all} = PS_{u,influx} \times \frac{CL_{int}}{PS_{u,efflux} + CL_{int}} \quad (6)$$

where $PS_{u,influx}$ and $PS_{u,efflux}$ represent the membrane permeability clearance of the unbound drug for the influx and efflux process from outside and inside the cells, respectively, and CL_{int} represents the "exact" intrinsic clearance which includes metabolism and/or biliary excretion of the unbound drug. When the CL_{tot} is 1.51 l/h/kg, the $f_b \cdot CL_{int,all}$ is calculated to be 3.04 l/h/kg from eq. 6, assuming the hepatic blood flow rate is 3 l/h/kg. As shown in eq. 6, the $CL_{int,all}$ will be reduced in proportion to the decrease in $PS_{u,influx}$. In the presence of 1.2 and 3.0 μM CsA, the $PS_{u,influx}$ of CER fell to 66 and 44% of the control, respectively, when the hepatocytes were incubated in the presence of rat plasma (Fig. 2b), and, therefore, the in vivo $f_b \cdot CL_{int,all}$ is reduced to 2.01 and 1.34 l/h/kg (i.e., 66 and 44% of the control), which gives a predicted CL_H value of 1.20 and 0.93 l/h/kg, respectively, from eq. 5. This predicted CL_H is comparable with the CL_H observed in the present in vivo study (1.09 and 1.05 l/h/kg, respectively) (Table 1), suggesting that the pharmacokinetic interaction between CER and CsA in rats can be quantitatively explained by inhibition of the transporter-mediated uptake of CER.

In conclusion, the increased plasma concentration of CER in rats when coadministered with CsA can be quantitatively explained by inhibition of transporter-mediated uptake. The present study strongly suggests that the inhibition of the transporter-mediated uptake in the liver affects the drug disposition. Also, in humans, it is possible that inhibition of the transporter-mediated uptake of drugs may lead to a clinically relevant DDI.

Acknowledgments. We are grateful to Bayer AG and Bayer Yakuhin for kindly providing us with radiolabeled and unlabeled CER. We are grateful to Kazuya Maeda and Wakaba Yamashiro at the University of Tokyo for kindly providing us rat Oatp1a1-expressing HEK293 cells and for technical advice. We also appreciate Pharsight Corporation for providing us a license for WinNonlin as part of the Pharsight Academic License (PAL) program.

References

Backman JT, Kyrklund C, Neuvonen M, and Neuvonen PJ (2002) Gemfibrozil greatly increases plasma concentrations of cerivastatin. *Clin Pharmacol Ther* **72**:685–691.

Boberg M, Angerbauer R, Kanhai WK, Karl W, Kern A, Radtke M, and Steinke W (1998) Biotransformation of cerivastatin in mice, rats and dogs *in vivo*. *Drug Metab Dispos* **26**:640–652.

Cattori V, Hagenbuch B, Hagenbuch N, Stieger B, Ha R, Winterhalter KE, and Meier PJ (2000) Identification of organic anion transporting polypeptide 4 (Oatp4) as a major full-length isoform of the liver-specific transporter-1 (rlst-1) in rat liver. *FEBS Lett* **474**:242–245.

Charatan F (2001) Bayer decides to withdraw cholesterol lowering drug. *Br Med J* **323**:359.

Hagenbuch B and Meier PJ (2003) The superfamily of organic anion transporting polypeptides. *Biochim Biophys Acta* **1609**:1–18.

Hirayama M, Yoshimura Y, and Moriyasu M (2000) Carrier-mediated uptake of cerivastatin in primary cultured rat hepatocytes. *Xenobio Metab Dispos* **15**:219–225.

Hirota N, Ito K, Iwatsubo T, Green CE, Tyson CA, Shimada N, Suzuki H, and Sugiyama Y (2001) *In vitro/in vivo* scaling of alprazolam metabolism by CYP3A4 and CYP3A5 in humans. *Biopharm Drug Dispos* **22**:53–71.

Ishigami M, Tokui T, Komai T, Tsukahara K, Yamazaki M, and Sugiyama Y (1995) Evaluation of the uptake of pravastatin by perfused rat liver and primary cultured rat hepatocytes. *Pharm Res (NY)* **12**:1741–1745.

Ito K, Iwatsubo T, Kanamitsu S, Nakajima Y, and Sugiyama Y (1998a) Quantitative prediction of *in vivo* drug clearance and drug interactions from *in vitro* data on metabolism, together with binding and transport. *Annu Rev Pharmacol Toxicol* **38**:461–499.

Ito K, Iwatsubo T, Kanamitsu S, Ueda K, Suzuki H, and Sugiyama Y (1998b) Prediction of pharmacokinetics alterations caused by drug-drug interactions: metabolic interaction in the liver. *Pharmacol Rev* **50**:387–411.

Jacquemin E, Hagenbuch B, Stieger B, Wolkoff AW, and Meier PJ (1994) Expression cloning of a rat liver Na^+-independent organic anion transporter. *Proc Natl Acad Sci USA* **91**:133–137.

Kanamitsu S, Ito K, and Sugiyama Y (2000) Quantitative prediction of *in vivo* drug-drug interactions from *in vitro* data based on physiological pharmacokinetics: use of maximum unbound concentration of inhibitor at the inlet to the liver. *Pharm Res (NY)* **17**:336–343.

Kouzuki H, Suzuki H, Ito K, Ohashi R, and Sugiyama Y (1999) Contribution of organic anion transporting polypeptide to uptake of its possible substrates into rat hepatocytes. *J Pharmacol Exp Ther* **288**:627–634.

Lemaire M and Tillement JP (1982) Role of lipoproteins and erythrocytes in the *in vitro* binding and distribution of cyclosporin A in the blood. *J Pharm Pharmacol* **34**:715–718.

Lowry OH, Rosebrough NJ, Farr AL, and Randall RJ (1951) Protein measurement with the Folin phenol reagent. *J Biol Chem* **193**:265–275.

Meier PJ, Eckhardt U, Schroeder A, Hagenbuch B, and Stieger B (1997) Substrate specificity of sinusoidal bile acid and organic anion uptake systems in rat and human liver. *Hepatology* **26**:1667–1677.

Miyauchi S, Sawada Y, Iga T, Hanano M, and Sugiyama Y (1993) Comparison of the hepatic uptake clearances of fifteen drugs with a wide range of membrane permeabilities in isolated rat hepatocytes and perfused rat livers. *Pharm Res (NY)* **10**:434–440.

Moghadasian MH (1999) Clinical pharmacology of 3-hydroxy-3-methylglutaryl coenzyme A reductase inhibitors. *Life Sci* **65**:1329–1337.

Mück W, Mai I, Fritsche L, Ochmann K, Rohde G, Unger S, Johne A, Bauer S, Budde K, Roots I, et al. (1999) Increase in cerivastatin systemic exposure after single and multiple dosing in cyclosporin-treated kidney transplant recipients. *Clin Pharmacol Ther* **65**:251–261.

Mück W (2000) Clinical pharmacokinetics of cerivastatin. *Clin Pharmacokinet* **39**:99–116.

Mueck W, Frey R, Boix O, and Voith B (2001) Gemfibrozil/cerivastatin interaction. *AAPS Pharm Sci* **3** (**Suppl.**):abstract No. 3566.

Noé B, Hagenbuch B, Stieger B, and Meier PJ (1997) Isolation of multispecific organic anion and cardiac glycoside transporter from rat brain. *Proc Natl Acad Sci USA* **94**:10346–10350.

Partridge WM, Premachandra BN, and Fierer G (1985) Transport of thyroxine bound to human prealbumin into rat liver. *Am J Physiol* **248**:G545–G550.

Prueksaritanont T, Tang C, Qiu Y, Mu L, Subramanian R, and Lin JH (2002a) Effects of fibrates on metabolism of statins in human hepatocytes. *Drug Metab Dispos* **30**:1280–1287.

Prueksaritanont T, Zhao JJ, Ma B, Roadcap BA, Tang C, Qiu Y, Liu L, Lin JH, Pearson G, and Baillie TA (2002b) Mechanistic studies on metabolic interactions between gemfibrozil and statins. *J Pharmacol Exp Ther* **301**:1042–1051.

Schroeder A, Eckhardt U, Stieger B, Tynes R, Schteingart CD, Hofmann AF, Meier PJ, and Hagenbuch B (1998) Substrate specificity of the rat liver Na^+-bile salt cotransporter in *Xenopus laevis* oocytes and in CHO cells. *Am J Physiol* **274**:G370–G375.

Shitara Y, Hirano M, Sato H, and Sugiyama Y (2004) Gemfibrozil and its glucuronide inhibit the organic anion transporting polypeptide 2 (OATP2/OATP1B1: *SLC21A6*)-mediated hepatic uptake and CYP2C8-mediated metabolism of cerivastatin: analysis of the mechanism of the clinically relevant drug-drug interaction between cerivastatin and gemfibrozil. *J Pharmacol Exp Ther* **311**:228–236.

Shitara Y, Itoh T, Sato H, Li AP, and Sugiyama Y (2003) Inhibition of transporter-mediated hepatic uptake as a mechanism for drug-drug interaction between cerivastatin and cyclosporin A. *J Pharmacol Exp Ther* **304**:610–616.

Shitara Y, Sugiyama D, Kusuhara H, Kato Y, Abe T, Meier PJ, Itoh T, and Sugiyama Y (2002) Comparative inhibitory effects of different compounds on rat Oatp1 (*Slc21a1*)- and Oatp2 (*Slc21a5*)-mediated transport. *Pharm Res (NY)* **19**:159–163.

Yamazaki M, Suzuki H, Hanano M, Tokui T, Komai T, and Sugiyama Y (1993) Na^+-independent multispecific anion transporter mediates active transport of pravastatin into rat liver. *Am J Physiol* **264**:G36–G44.

Yamazaki M, Suzuki H, and Sugiyama Y (1996) Recent advances in carrier-mediated hepatic uptake and biliary excretion of xenobiotics. *Pharm Res (NY)* **13**:497–513.

Wang J-S, Neuvonen M, Wen X, Backman JT, and Neuvonen PJ (2002) Gemfibrozil inhibits CYP2C8-mediated cerivastatin metabolism in human liver microsomes. *Drug Metab Dispos* **30**:1352–1356.

Address correspondence to: Dr. Yuichi Sugiyama, Department of Molecular Pharmacokinetics, Graduate School of Pharmaceutical Sciences, The University of Tokyo, 7-3-1, Hongo, Bunkyo-ku, Tokyo 113-0033, Japan. E-mail: sugiyama@mol.f.u-tokyo.ac.jp

Transporter Database, TP-Search: A Web-Accessible Comprehensive Database for Research in Pharmacokinetics of Drugs

This Letter to the Editor informs the readers of TP-Search, a unique comprehensive database for membrane transporter proteins that we have constructed to facilitate the study of drug transporters on a broad scale in the world and to provide a research tool for optimization of pharmacokinetic properties in terms of transporters during the early stage of drug development in pharmaceutical companies.

During the past decade, there has been a significant increase in the molecular characterization of transporter proteins in animals and humans (1). With newer information on the genetic/genomic studies, this has led to a better understanding of the importance of such transporter proteins as one of the main determinant factors to play a key role in drug disposition; that is, absorption, distribution, and excretion (ADE) of drugs (2–4). Because the amount of available data is rapidly increasing, a need for a publicly accessible database with comprehensive information about all of the known membrane transporters becomes increasingly important.

We have constructed TP-Search, a Web-accessible relational database on ADE-associated transporter proteins (http://www.tp-search.jp/), enabling users to search dynamically transporter-related information by chemical structures/names of substrate/inhibitor/inducers, gene expression, functions, drug-drug interaction involving transporters, and so on.

The other databases on transporters, which are currently available, are http://nutrigen.4t.com/humanabc.htm (database on ABC transporters by M. Müller), http://www.med.rug.nl/mdl/ (database of University Hospital Groningen), http://www.gene.ucl.ac.uk/nomenclature/genefamily/abc.html (HGNC gene family nomenclature ABC transporters), http://lab.digibench.net/transporter/ (human membrane transporter database), http://xin.cz3.nus.edu.sg/group/adment/adment.asp (ADME-associated proteins database), and http://www.mhc.com/PGP/index.html (P-glycoprotein interaction). These have appeared to provide only certain aspects of specific class or group of membrane transporter proteins, whereas TP-Search aims at providing a comprehensive database on drug-transporters. Among those databases, the human membrane transporter database has been intended to support pharmacogenomic studies and so provides much information on sequence variants, altered functions caused by polymorphisms/mutations, and (patho)physiological role and associated diseases (5). The ADME-associated protein database provides comprehensive information on ADME-associated proteins, which include not only membrane transporter proteins involved in drug disposition, but also other proteins, such as plasma proteins, intracellular binding proteins, and drug metabolizing enzymes (6). Other transporter databases listed above are mainly focused on the information for ABC-transporters.

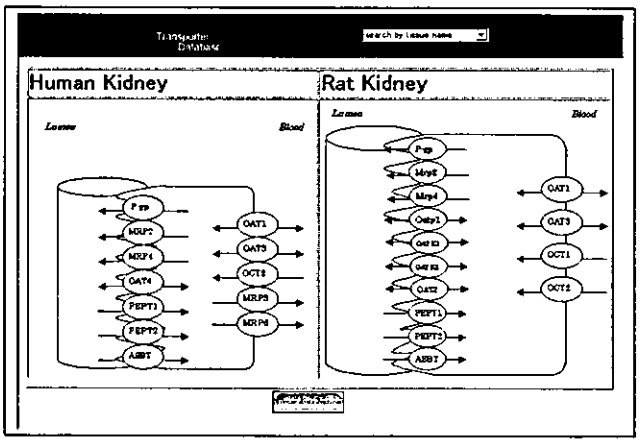

Fig. 1. Example of search results on transporters expressed in human and rat kidney.

Our methodology was as follows. Membrane transporter proteins were selected from a comprehensive search of available literature consisting of research papers, review articles, pharmacology textbooks, and other relevant publications (via PubMed; http://www.ncbi.nlm.gov/PubMed/), resulting in approximately 1,940 articles published from 1968 to 2002. The system is a typical Web application built on Application server, Web server, and Relational Database Management System (RDMS) to provide the services via the Internet. The user connects with the URL at http://www.tp-search.jp/ by a Web browser such as Netscape Navigator or Microsoft Internet Explorer.

The database, TP-Search, contains information on more than 75 membrane transporters (Table I), including cDNA and amino acid sequences, gene family, putative membrane topology, driving force, transport direction, substrate/inhibitor/inducer (chemical structures and kinetic data, i.e., Km/Ki), and tissue distribution in humans as well as in mice and rats, and drug-drug interactions involving transporters. All information available in this database is linked to the original references in PubMed, which ensures the users can confirm the validity of data and to obtain more detailed information available in the original references.

Terminology regarding genes often causes confusion. In our database, we use primarily the "Nomenclature of Mammalian Transporter Genes," (http://www.gene.ucl.ac.uk/cgi-bin/nomenclature/searchgenes.pl/), such as the solute carrier superfamily (SLC) and ATP-binding cassette transporters (ABC). These standardized gene names, accompanied by conventional names, are both given in this database. The sequential information for transporters posted in the database was available through "Locus-Link" (http://www.ncbi.nlm.nih.gov/LocusLink/), and names and structures of the compounds, such as substrates/inhibitors/inducers, were searched through "Chem-Link" and "Japanese Accepted Names for Pharmaceuticals" (http://moldb.nihs.go.jp/jan/).

TP-Search is searchable by transporter name, tissue name (liver, kidney, intestine, brain, and expression in cell line; Fig. 1), substrate/inhibitor/inducer name, and drug-drug interaction. Implemented as a relational database, searches involving any combination of these options or selection field are also supported.

Because drug transporters have demonstrated a broad substrate specificity, drug-drug interaction involving these transporters is considered very likely. Approximately 1,200

0724-8741/04/1100-2133/0

Table I. Membrane Transporters Archived in TP-Search

Transporters	Human	Mouse	Rat
P-glycoprotein (MDR)	MDR1	Mdr1a, Mdr1b	Mdr1a, Mdr1b
Multidrug resistance-associated protein	MRP1, MRP2, MRP3, MRP4, MRP5, MRP6	Mrp1, Mrp2, Mrp5	Mrp1, Mrp2, Mrp3, Mrp6
Breast cancer resistant protein	BCRP	Bcrp	Bcrp
Bile salt export pump	BSEP	Bsep	Bsep
Organic anion transporting polypeptide	OATP-A, OATP-B, OATP-C, OATP-D, OATP-E, OATP-8, PGT	Oatp1, Oatp2, Oatp4, Oatp5, Pgt	Oatp1, Oatp2, Oatp3, Oatp4, OAT-K1, OAT-K2, Pgt
Bile acid transporter	NTCP, ASBT	Ntcp, Asbt	Ntcp, Asbt
Organic anion transporter	OAT1, OAT2, OAT3, OAT4	OAT1, OAT2, OAT3	OAT1, OAT2, OAT3
Organic cation transporter	OCT1, OCT2, OCT3	OCT1, OCT2, OCT3	OCT1, OCT2, OCT3
Organic cation/carnitine transporter	OCTN1, OCTN2	OCTN1, OCTN2, OCTN3	OCTN1, OCTN2
Peptide transporter	PEPT1, PEPT2	PEPT1, PEPT2	PEPT1, PEPT2

compounds known as substrates/inhibitors/inducers, including their names and structures, are currently archived in this database. With respect to the information currently available in this database, the exact role of transporter proteins in the observed *in vivo* drug-drug interaction has not always been clearly defined. It might be just extrapolated from *in vitro* information, such as substrate affinity, inhibitory effect, and so forth. In addition, because the substrate specificity of CYP3A and P-glycoprotein overlaps, many drugs may be a substrate of both (7,8). In such cases, it is difficult to distinguish the contribution to the increased oral bioavailability between CYP3A and P-glycoprotein. When the role of transporter proteins in the *in vivo* drug-drug interaction was suggested or indicated in peer-reviewed references, such information was incorporated into this database, even though there might be the limitation of scientific validity of such data.

This database will be updated periodically (bimonthly or quarterly), so that information regarding newly identified ADE-associated membrane transport proteins and additional knowledge about function or related proteins will be added. Toward that end, a data submission interface will be available in the database.

Naoki Ozawa[1,2]
Takako Shimizu[2]
Rika Morita[2]
Yoshiya Yokono[2]
Takafumi Ochiai[2]
Kiyotaka Munesada[2]
Akira Ohashi[2]
Yoshitaka Aida[2]
Yoshimasa Hama[2]
Katsuhiko Taki[3]
Kazuya Maeda[4]
Hiroyuki Kusuhara[4]
and Yuichi Sugiyama[4]
[1]*Wyeth K.K., Tokyo*
[2]*Advanced Research Institute for Science and Engineering, Waseda University, Tokyo*
[3]*Nihon Visual Science, Inc., Tokyo*
[4]*Graduate School of Pharmaceutical Science, The University of Tokyo, Tokyo*

Received November 30, 2003; accepted July 23, 2004

REFERENCES

1. R. B. Kim. Transporters in drug disposition. *Curr. Opin. Drug Discov. Devel.* **3**:94–101 (2000).
2. V. H. Lee, J. L. Sporty, and T. E. Fandy. Pharmacogenomics of drug transporters: the next drug delivery challenge. *Adv. Drug Deliv. Rev.* **50**:S33–S40 (2001).
3. A. Ayrton and P. Morgan. Role of transport proteins in drug absorption, distribution and excretion. *Xenobiotica* **31**:469–497 (2001).
4. H. Kusuhara and Y. Sugiyama. Role of transporters in the tissue-selective distribution and elimination of drugs: transporters in the liver, small intestine, brain and kidney. *J. Controlled Release* **78**: 43–54 (2002).
5. Q. Yan and W. Sadée. Human membrane transporter database: A web-accessible relational database for drug transport studies and pharmacogenomics. *AAPS Pharmsci.* **2**: 1–7 (2000).
6. L. Z. Ji Sun, X. Chen, J. F. Wang, and Y. Z. Chen. ADME-AP: a database of ADME associated proteins. *Bioinformatics* **18**: 1699–1700 (2002).
7. H. Suzuki and Y. Sugiyama. Role of metabolic enzymes and efflux transporters in the absorption of drugs from the small intestine. *Eur. J. Pharm. Sci.* **12**:3–12 (2000).
8. V. J. Wacher, L. Salphati, and L. Z. Benet. Active secretion and enterocytic drug metabolism barriers to drug absorption. *Adv. Drug Deliv. Rev.* **46**:89–102 (2001).

0022-3565/04/3111-139–146$20.00
THE JOURNAL OF PHARMACOLOGY AND EXPERIMENTAL THERAPEUTICS

JPET 311:139–146, 2004

Vol. 311, No. 1
68056/1168312
Printed in U.S.A.

Contribution of OATP2 (OATP1B1) and OATP8 (OATP1B3) to the Hepatic Uptake of Pitavastatin in Humans

Masaru Hirano, Kazuya Maeda, Yoshihisa Shitara, and Yuichi Sugiyama

Graduate School of Pharmaceutical Sciences, The University of Tokyo, Tokyo, Japan (M.H., K.M., Y.Su.); and School of Pharmaceutical Sciences, Showa University, Tokyo, Japan (Y.Sh.)

Received March 8, 2004; accepted May 24, 2004

ABSTRACT

Pitavastatin, a novel potent 3-hydroxymethylglutaryl-CoA reductase inhibitor, is selectively distributed to the liver in rats. However, the hepatic uptake mechanism of pitavastatin has not been clarified yet. In the present study, we investigated the contribution of organic anion transporting polypeptide 2 (OATP2/OATP1B1) and OATP8 (OATP1B3) to pitavastatin uptake using transporter-expressing HEK293 cells and human cryopreserved hepatocytes. Uptake studies using OATP2- and OATP8-expressing cells revealed a saturable and Na^+-independent uptake, with K_m values of 3.0 and 3.3 μM for OATP2 and OATP8, respectively. To determine which transporter is more important for its hepatic uptake, we proposed a methodology for estimating their quantitative contribution to the overall hepatic uptake by comparing the uptake clearance of pitavastatin with that of reference compounds (a selective substrate for OATP2 (estrone-3-sulfate) and OATP8 (cholecystokinin octapeptide) in expression systems and human hepatocytes. The concept of this method is similar to the so-called relative activity factor method often used in estimating the contribution of each cytochrome P450 isoform to the overall metabolism. Applying this method to pitavastatin, the observed uptake clearance in human hepatocytes could be almost completely accounted for by OATP2 and OATP8, and about 90% of the total hepatic clearance could be accounted for by OATP2. This result was also supported by estimating the relative expression level of each transporter in expression systems and hepatocytes by Western blot analysis. These results suggest that OATP2 is the most important transporter for the hepatic uptake of pitavastatin in humans.

Pitavastatin is a highly potent inhibitor of 3-hydroxy-3-methylglutaryl (HMG)-CoA reductase, the rate-limiting enzyme in cholesterol biosynthesis (Aoki et al., 1997; Kajinami et al., 2003). Previously, Kimata et al. (1998) have demonstrated that [^{14}C]pitavastatin is selectively distributed to the liver in rats with the liver/plasma concentration ratio of more than 53. Shimada et al. (2003) have recently reported that the uptake of pitavastatin by rat hepatocytes is saturable and temperature dependent, suggesting that pitavastatin might be transported by carrier-mediated systems. Pitavastatin is scarcely metabolized in human liver microsomes (Fujino et al., 2003) and is excreted into the bile in unchanged form (Kojima et al., 2001). In humans, the fraction excreted in urine was less than 2% (Kajinami et al., 2003). Therefore, when considering the pharmacokinetics of pitavastatin, we should focus on the hepatic clearance of unchanged pitavastatin.

Statins reduce the plasma level of low-density lipoprotein cholesterol and triglycerides in a dose-dependent manner, whereas one of the severe adverse effects, rhabdomyolysis, also appears to be dose-dependent (Davidson et al., 1997). Since liver is a major clearance organ as well as a pharmacological target organ of pitavastatin, it is essential to clarify the uptake mechanism of pitavastatin by hepatocytes to predict the pharmacological and toxicological effects.

At the present time, several transporters are thought to be involved in the hepatic uptake of a variety of drugs in human liver. Na^+-taurocholate cotransporting polypeptide, organic anion transporting polypeptide (OATP) 2 (OATP1B1, OATP-C/LST-1), OATP8 (OATP1B3, LST-2), OATP-B (OATP2B1), organic anion transporter (OAT) 2, and organic cation transporter 1 are localized on the basolateral membrane of human hepatocytes (Hagenbuch and Meier, 1996, 2003; Muller and Jansen, 1997). In particular, OATP2 and OATP8 are selectively expressed in the human liver and exhibit broad sub-

This study was supported by Health and Labor Sciences Research grants from the Ministry of Health, Labor, and Welfare for the Research on Advanced Medical Technology and by Grant-in Aid for Young Scientists B 15790087 from the Ministry of Education, Culture, Sports, Science, and Technology.
Article, publication date, and citation information can be found at http://jpet.aspetjournals.org.
doi:10.1124/jpet.104.068056.

ABBREVIATIONS: HMG, 3-hydroxy-3-methylglutaryl; OATP, organic anion transporting polypeptide; $E_2$17βG, estradiol 17β-D-glucuronide; E-sul, estrone-3-sulfate; CCK-8, cholecystokinin octapeptide; PCR, polymerase chain reaction; TBS-T, Tris-buffered saline containing 0.05% Tween 20; RAF, relative activity factor; CL, clearance.

strate specificities, which suggest that they play an important role in the hepatic uptake of several anionic endogenous compounds and drugs (Hagenbuch and Meier, 2003). OATP2 accepts statins including pravastatin, cerivastatin, and rosuvastatin as substrates (Hsiang et al., 1999; Brown et al., 2001; Nakai et al., 2001; Sasaki et al., 2002; Shitara et al., 2003a). The substrate specificity of OATP2 commonly overlaps that of OATP8, and several compounds can be bisubstrates of both OATP2 and OATP8. However, there are some differences as far as substrate recognition and transcriptional regulation are concerned (Hagenbuch and Meier, 2003; Kullak-Ublick et al., 2004). Therefore, it is essential to evaluate their quantitative contribution to the total hepatic uptake to estimate the overall hepatic clearance for individuals when there are changes in expression level or function caused by pathological conditions, single-nucleotide polymorphisms, and transporter-mediated drug-drug interactions. This kind of information will help us predict the distribution of pitavastatin in the target organ, as well as the plasma concentrations, subsequent pharmacological effects, and adverse events under these conditions. However, so far, no studies have been published describing how to estimate the contribution of each uptake transporter quantitatively in human liver.

In the present study, we analyzed the involvement of the transporters, OATP2 and OATP8, in the hepatic uptake of pitavastatin along with estradiol 17β-D-glucuronide ($E_2$17βG), a typical substrate of both OATP2 and OATP8 (Cui et al., 2001; Ismair et al., 2001). In addition, we developed a methodology for determining the contribution of each transporter to the hepatic uptake of test compounds by comparing their uptake clearance with that of reference compounds (a selective substrate for OATP2 (estrone-3-sulfate) and OATP8 (cholecystokinin octapeptide) in expression systems and human hepatocytes. We also used another approach by directly comparing expression levels of OATP2 and OATP8 in expression systems and hepatocytes using Western blot analysis and compared the results obtained by these two methods.

Materials and Methods

Materials. Pitavastatin (monocalcium bis[(3R,5S,6E)-7-[2-cyclopropyl-4-(4-fluorophenyl)-3-quinolyl]3,5-dihydroxy-6-hepteonate]) was synthesized by Nissan Chemical Industries (Chiba, Japan). [Fluorobenzene-*U*-^{14}C]pitavastatin (11.7 mCi/mmol) was synthesized by Amersham Biosciences UK, Ltd. (Little Chalfont, Buckinghamshire, UK). $E_2$17βG and estrone-3-sulfate (E-sul) (45 and 46 Ci/mmol, respectively) were purchased from PerkinElmer Life and Analytical Sciences (Boston, MA), whereas cholecystokinin octapeptide (CCK-8) (77 Ci/mmol) was purchased from Amersham Biosciences UK, Ltd.. Unlabeled $E_2$17βG, E-sul, and CCK-8 were purchased from Sigma-Aldrich (St. Louis, MO). All other chemicals were of analytical grade and commercially available.

Construction of Stably Transfected HEK293 Cells Expressing Human OATP2 and OATP8. The human OATP2 gene was isolated by PCR using the human liver cDNA purchased from Takara Bio Inc. (Shiga, Japan). The first half (1–1125) of the gene was amplified using a forward primer containing a KpnI site (5′-GGGGTACCATGGACCAAAATCAACATTTGAAT-3′) and a reverse primer (5′-GTTAGCCTTAGATGAAGGCTGACC-3′). The second half (1041–2076) of the gene was amplified using a forward primer (5′-ACAAGTAAGCAGCTATATTGGTGC-3′) and a reverse primer containing a NotI site (5′-GGGCGGCCGCTTAACAATGTGTTTCACTATCTG-3′). Each PCR product was TA cloned into the pGEM vector (Promega, Madison, WI), respectively. Then, the pGEM vector containing the first half was digested with KpnI and Eco105 I, and the pGEM vector with the second half was digested with Eco105 I and NotI. Subsequently, the first and second halves of the OATP2 cDNA were ligated into KpnI and NotI sites of the pcDNA3.1 (+) (Invitrogen, Carlsbad, CA) to obtain the full-length human OATP2 gene.

The human OATP8 gene was isolated by PCR using human liver cDNA purchased from BD Biosciences Clontech (Palo Alto, CA) as a template. The C-terminal fragment of the OATP8 gene was amplified using a forward primer (5′-AGAGTCAGCATCTTCAGAG-3′) and a reverse primer (5′-TTTTCCTTTTGCGGCCGCATTGTCAGTGAAAGACCAGG-3′) and TA cloned into pGEM vector. The N-terminal fragment was amplified using a forward primer containing a HindIII site and Kozak sequence just before the start codon (5′-CCCAAGCTTCCGCCATGGACCAACATCAAC-3′) and a reverse primer (5′-CTTCGGTCTGTGTAGTTTAG-3′). To subclone the full length of the OATP8 cDNA, fragment 1 was prepared by digesting the pGEM vector containing the C-terminal fragment with HindIII and NotI, and fragment 2 was created by digesting the pGEM vector containing the N-terminal fragment with HindIII. Then, fragments 1 and 2 were ligated into linearized pcDNA3.1 (+) digested with HindIII and NotI.

OATP2- and OATP8-expressing HEK293 cells and control cells were constructed by the transfection of expression vector and control pcDNA3.1 vector, respectively, into cells using FuGENE6 (Roche Diagnostics, Indianapolis, IN), according to the manufacturer's instruction and the selection by 800 μg/ml Antibiotic G418 sulfate (Promega, Madison, WI) for 3 weeks.

Cell Culture. Transporter-expressing or vector-transfected HEK293 cells were grown in Dulbecco's modified Eagle's medium low glucose (Invitrogen) supplemented with 10% fetal bovine serum (Sigma-Aldrich), 100 U/ml penicillin, 100 μg/ml streptomycin, and 0.25 μg/ml amphotericin B at 37°C with 5% CO_2 and 95% humidity. Cells were then seeded in 12-well plates at a density of 1.5×10^5 cells/well. For the transport study, the cell culture medium was replaced with culture medium supplemented with 5 mM sodium-butyrate for 24 h before transport assay to induce the expression of OATP2 and OATP8.

Transport Study Using Transporter Expression Systems. The transport study was carried out as described previously (Sugiyama et al., 2001). Uptake was initiated by adding Krebs-Henseleit buffer containing radiolabeled and unlabeled substrates after cells had been washed twice and preincubated with Krebs-Henseleit buffer at 37°C for 15 min. The Krebs-Henseleit buffer consisted of 118 mM NaCl, 23.8 mM $NaHCO_3$, 4.8 mM KCl, 1.0 mM KH_2PO_4, 1.2 mM $MgSO_4$, 12.5 mM HEPES, 5.0 mM glucose, and 1.5 mM $CaCl_2$ adjusted to pH 7.4. The uptake was terminated at a designated time by adding ice-cold Krebs-Henseleit buffer after removal of the incubation buffer. Then, cells were washed twice with 1 ml of ice-cold Krebs-Henseleit buffer, solubilized in 500 μl of 0.2 N NaOH, and kept overnight at 4°C. Aliquots (500 μl) were transferred to scintillation vials after adding 250 μl of 0.4 N HCl. The radioactivity associated with the cells and incubation buffer was measured in a liquid scintillation counter (LS6000SE; Beckman Coulter, Fullerton, CA) after adding 2 ml of scintillation fluid (Clear-sol I; Nacalai Tesque, Kyoto, Japan) to the scintillation vials. The remaining 50 μl of cell lysate was used to determine the protein concentration by the method of Lowry with bovine serum albumin as a standard.

Transport Study Using Human Cryopreserved Hepatocytes. This experiment was performed as described previously (Shitara et al., 2003a). Cryopreserved human hepatocytes were purchased from In Vitro Technologies (Baltimore, MD). In this experiment, we selected three batches of human hepatocytes (Lot. OCF, 094, and ETR) that show relatively high uptake amount of $E_2$17βG and E-sul among eight independent batches of hepatocytes. Immediately before the study, the hepatocytes (1-ml suspension) were thawed at 37°C, then quickly suspended in 10 ml of ice-cold Krebs-Henseleit buffer and centrifuged (50*g*) for 2 min at 4°C, followed by

removal of the supernatant. This procedure was repeated once more to remove cryopreservation buffer, and then the cells were resuspended in the same buffer to give a cell density of 1.0×10^6 viable cells/ml for the uptake study. The number of viable cells was determined by trypan blue staining. To measure the uptake in the absence of Na^+, sodium chloride and sodium bicarbonate in Krebs-Henseleit buffer were replaced with choline chloride and choline bicarbonate. Prior to the uptake studies, the cell suspensions were prewarmed in an incubator at 37°C for 3 min. The uptake studies were initiated by adding an equal volume of buffer containing labeled and unlabeled substrates to the cell suspension. After incubation at 37°C for 0.5, 2, or 5 min, the reaction was terminated by separating the cells from the substrate solution. For this purpose, an aliquot of 80 μl of incubation mixture was collected and placed in a centrifuge tube (450 μl) containing 50 μl of 2 N NaOH under a layer of 100 μl of oil (density, 1.015, a mixture of silicone oil and mineral oil; Sigma-Aldrich), and subsequently the sample tube was centrifuged for 10 s using a tabletop centrifuge (10,000*g*, Beckman Microfuge E; Beckman Coulter). During this process, hepatocytes passed through the oil layer into the alkaline solution. After an overnight incubation in alkali to dissolve the hepatocytes, the centrifuge tube was cut and each compartment was transferred to a scintillation vial. The compartment containing the dissolved cells was neutralized with 50 μl of 2 N HCl, mixed with scintillation cocktail, and the radioactivity was measured in a liquid scintillation counter.

Antiserum and Western Blot Analysis. As shown in previous reports, anti-OATP2 and anti-OATP8 sera were raised in rabbits against a synthetic peptide consisting of the 21 and 15 carboxyl-terminal amino acids, respectively, of OATP2 and OATP8 coupled to keyhole limpet hemocyanine at its N terminus via an additional cysteine (Konig et al., 2000a,b). Crude membrane fractions were prepared from human hepatocytes and transporter-expressing HEK293 cells as described previously (Sasaki et al., 2002). The crude membrane fractions were diluted with 3× Red loading buffer (Bio-Labs, Hertfordshire, UK) and loaded onto a 7% SDS-polyacrylamide gel with a 4.4% stacking gel. Proteins were electroblotted onto a polyvinylidene diflouride membrane (Pall, East Hills, NY) using a blotter (Trans-blot; Bio-Rad, Hercules, CA) at 15 V for 1 h. The membrane was blocked with Tris-buffered saline containing 0.05% Tween 20 (TBS-T) and 5% skimmed milk for 1 h at room temperature. After washing with TBS-T, the membrane was incubated with anti-OATP2 serum (dilution 1:500) or anti-OATP8 serum (dilution 1:1000). The membrane was incubated with a horseradish peroxidase-labeled anti-rabbit IgG antibody (Amersham Biosciences UK, Ltd.) diluted 1:2000 in TBS-T for 1 h at room temperature followed by washing with TBS-T. The band was detected, and its intensity was quantified using an image analyzer (LAS-1000 plus; Fuji Film, Tokyo, Japan).

Kinetic Analyses. Ligand uptake was expressed as the uptake volume (microliters per milligram of protein), given as the amount of radioactivity associated with the cells (disintegrations per minute per milligram of protein) divided by its concentration in the incubation medium (disintegrations per minute per microliter). Specific uptake was obtained by subtracting the uptake into vector-transfected cells from the uptake into cDNA-transfected cells. Kinetic parameters were obtained using the following equation:

$$v = \frac{V_{max} \times S}{K_m + S} + P_{dif} \times S \quad (1)$$

where v is the uptake velocity of the substrate (picomoles per minute per milligram of protein), S is the substrate concentration in the medium (micromolar), K_m is the Michaelis constant (micromolar), V_{max} is the maximum uptake rate (picomoles per minute per milligram of protein), and P_{dif} is the nonsaturable uptake clearance (microliters per minute per milligram of protein). Fitting was performed by the nonlinear least-squares method using a MULTI program (Yamaoka et al., 1981), and the Damping Gauss Newton Method algorithm was used for fitting. The input data were weighted as the reciprocal of the observed values.

To determine saturable hepatic uptake clearance in human hepatocytes, we first determined the hepatic uptake clearance [$CL_{(2min-0.5min)}$] (microliters per minute per 10^6 cells) by calculating the slope of the uptake volume (V_d) (microliters per 10^6 cells) between 0.5 and 2 min (eq. 2). The saturable component of the hepatic uptake clearance (CL_{hep}) was determined by subtracting $CL_{(2\ min-0.5\ min)}$ in the presence of 100 μM substrate (excess) from that in the presence of 1 μM substrate (tracer) (eq. 3).

$$CL_{(2\ min\ -\ 0.5\ min)} = \frac{V_{d,2\ min} - V_{d,0.5\ min}}{2 - 0.5} \quad (2)$$

$$CL_{hep} = CL_{(2\ min\ -\ 0.5\ min),tracer} - CL_{(2\ min\ -\ 0.5\ min),excess} \quad (3)$$

where $CL_{(2min-0.5min),tracer}$ and $CL_{(2min-0.5\ min),excess}$ represent $CL_{(2min-0.5min)}$ estimated in the presence of 1 and 100 μM substrate, respectively.

Estimation of Uptake Clearance in Human Hepatocytes from cDNA Transfectants. The use of this method for estimating the contribution of each molecule to the overall reaction [relative activity factor (RAF) method] has been described for cytochrome P450 (Crespi and Penman, 1997), and it has also been applied to renal uptake transporters (Håsegawa et al., 2003). Based on this strategy, we estimated the contribution of OATP2 and OATP8 to the overall uptake by human hepatocytes. Because E-sul and CCK-8 could be selective substrates for OATP2 and OATP8, respectively, they were used as reference compounds for OATP2- and OATP8-mediated uptake (Cui et al., 2001; Ismair et al., 2001). The ratio of the uptake clearance of reference compounds in human hepatocytes to that in the expression system was calculated and defined as $R_{act,\ OATP2}$ and $R_{act,\ OATP8}$. The uptake clearance by OATP2 and OATP8 was separately calculated by multiplying the uptake clearance of the test compounds (pitavastatin and $E_2 17\beta G$) in transporter-expressing cells ($CL_{OATP2,test}$ and $CL_{OATP8,test}$) by $R_{act,\ OATP2}$ and $R_{act,\ OATP8}$, respectively, as described in the following equations:

$$R_{act,OATP2} = \frac{CL_{Hep,E-sul}}{CL_{OATP2,E-sul}} \quad (4)$$

$$R_{act,OATP8} = \frac{CL_{Hep,CCK-8}}{CL_{OATP8,CCK-8}} \quad (5)$$

$$CL_{hep,test,OATP2} = CL_{OATP2,test} \cdot R_{act,OATP2} \quad (6)$$

$$CL_{hep,test,OATP8} = CL_{OATP8,test} \cdot R_{act,OATP8} \quad (7)$$

$$CL_{hep,test} = CL_{hep,test,OATP2} + CL_{hep,test,OATP8} \quad (8)$$

In addition, the ratio of the expression levels of OATP2 and OATP8 in human hepatocytes (per 10^6 cells) to transporter-expressing cells (per milligram of protein) ($R_{exp,\ OATP2}$ and $R_{exp,\ OATP8}$) could be calculated from the intensity of specific bands in Western blot analysis and the amount of crude membrane prepared from each cell type as follows. The relative expression level per 10^6 hepatocytes or milligram of protein in HEK293 whole cells was given by multiplying the band density per unit protein amount in crude membrane of each batch of hepatocytes or transporter-expressing HEK293 cells by protein amount in crude membrane obtained by 10^6 hepatocytes or 1 mg of whole-cell protein in HEK293 transfectants. The R_{exp} value was calculated as the relative expression level per 10^6 hepatocytes divided by that per milligram of protein in HEK293 cells. The OATP2- and OATP8-mediated hepatic uptake of test compounds (pitavastatin and $E_2 17\beta G$) was calculated from the following equation:

$$CL_{hep,test} = CL_{OATP2,test} \cdot R_{exp,OATP2} + CL_{OATP8,test} \cdot R_{exp,OATP8} \quad (9)$$

Results

Uptake of $E_2$17βG, E-sul, CCK-8, and Pitavastatin by Transporter-Expressing Cells. The saturation kinetics of $E_2$17βG, E-sul, CCK-8, and pitavastatin by OATP2- and OATP8-expressing cells and vector-transfected HEK293 are shown as Eadie-Hofstee plots in Fig. 1. Pitavastatin as well as $E_2$17βG were significantly taken up into both OATP2- and OATP8-expressing HEK293 cells compared with vector-transfected cells (Fig. 1, A and D). The transfection of OATP2 resulted in an increase in the uptake of E-sul but did not affect the uptake of CCK-8, whereas transfection of OATP8 resulted in an increase in the uptake of CCK-8 but not E-sul (Fig. 1, B and C). The concentration dependence of the uptake of pitavastatin, $E_2$17βG, and E-sul could be explained by a one-saturable component (Fig. 1, A, B, and D). However, a saturable and a nonsaturable component could be accounted for even in the specific uptake of CCK-8 determined by subtraction of the uptake by vector-transfected cells from that by OATP8-expressing cells (Fig. 1C). Their kinetic parameters are summarized in Table 1. The rank order in the uptake clearance by OATP2 was E-sul > pitavastatin > $E_2$17βG, whereas that by OATP8 was pitavastatin > CCK-8 > $E_2$17βG.

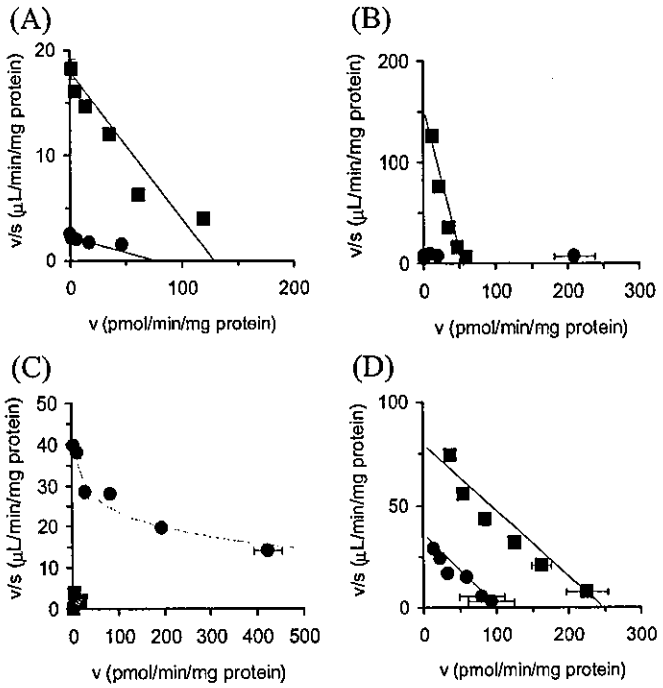

Fig. 1. Eadie-Hofstee plots of the uptake of [^{3}H]$E_2$17βG, [^{3}H]E-sul, [^{3}H]CCK-8, and [^{14}C]pitavastatin by OATP2- and OATP8-expressed HEK293 cells. Squares and circles represent the uptake in OATP2- and OATP8-expressed cells, respectively. The concentration dependence of OATP2- and OATP8-mediated uptake of [^{3}H]$E_2$17βG (A), [^{3}H]E-sul (B), [^{3}H]CCK-8 (C), and [^{14}C]pitavastatin (D) is shown as Eadie-Hofstee plots. The uptake of [^{3}H]$E_2$17βG, [^{3}H]E-sul, [^{3}H]CCK-8, and [^{14}C]pitavastatin for 5, 0.5, 2, and 2 min, respectively, was determined at various concentrations (0.1–30 μM). The OATP2- and OATP8-mediated transport was obtained by subtracting the uptake in vector-transfected cells from that in OATP2- or OATP8-expressing cells. Lines represent the fitted curves obtained by nonlinear regression analysis. Each point represents the mean ± S.E. (n = 3).

Uptake of $E_2$17βG, E-sul, CCK-8, and Pitavastatin by Human Cryopreserved Hepatocytes. Typical time profiles of the uptake of $E_2$17βG, E-sul, CCK-8, and pitavastatin in one batch of human hepatocytes (Lot. OCF) are shown in Fig. 2. Time-dependent uptake of all ligands was observed at 1 μM, and it was decreased in the presence of 100 μM unlabeled ligands in all batches of hepatocytes examined in the present study (data not shown). The uptake clearance of these substrates in each donor is listed in Table 2. The uptake clearance by human hepatocytes was in the order E-sul > pitavastatin > $E_2$17βG > CCK-8.

The Effect of Sodium Ion on the Uptake of Pitavastatin by Human Cryopreserved Hepatocytes. To determine whether the uptake of pitavastatin into hepatocytes is Na^+ dependent or not, we investigated the pitavastatin uptake in the presence and absence of Na^+ in human hepatocytes. As shown in Fig. 3, replacement of Na^+ with choline in the transport buffer had no effect on the uptake of pitavastatin in human hepatocytes.

Western Blot Analysis. The relative expression levels of OATP2 and OATP8 in crude membrane from transfected cells and hepatocytes were investigated by Western blot analyses. An antiserum against OATP2 recognized approximately 80-kilodalton proteins in the crude membrane fractions prepared from human hepatocytes and OATP2-expressing cells, respectively (Fig. 4A). Anti-OATP8 antiserum could detect the specific band of approximately 120-kilodalton proteins in the crude membrane fractions prepared from human hepatocytes and OATP8-expressing cells, respectively (Fig. 4B). The molecular weights of OATP2 and OATP8 in the human hepatocytes were almost the same as those in OATP2- and OATP8-expressing cells, respectively. No expression of OATP2 or OATP8 was observed in vector-transfected HEK293 cells (Fig. 4, A and B). Figure 4, C and D showed the linear relationship between the applied amount of crude membrane obtained from transporter-expressing cells and human hepatocytes and the intensity of the specific band measured by digital densitometer. The slope of the

TABLE 1

Kinetic parameters of the uptake of compounds by transporter-expressing HEK293 cells

Data shown in Fig. 1 were used to determine these parameters calculated by nonlinear regression analysis. Each point represents the mean ± S.E. (n = 3).

Transporter	Substrate	K_m	V_{max}	V_{max}/K_m	P_{dif}
		μM	pmol/min/mg	μl/min/mg	μl/min/mg
OATP2	E-sul	0.458 ± 0.154	60.3 ± 8.8	132 ± 19	
	CCK-8		Not significantly transported		
	Pitavastatin	3.00 ± 0.39	230 ± 17	76.6 ± 5.6	
	$E_2$17βG	8.29 ± 0.42	131 ± 5	15.8 ± 0.6	
OATP8	E-sul		Not significantly transported		
	CCK-8	3.82 ± 2.20	102 ± 60	26.7 ± 15.7	11.4 ± 2.6
	Pitavastatin	3.25 ± 0.44	100 ± 8	30.6 ± 2.3	
	$E_2$17βG	24.6 ± 7.6	56.8 ± 16.1	2.31 ± 0.65	

P_{dif} nonsaturable uptake clearance (microliters per minute per milligram of protein).

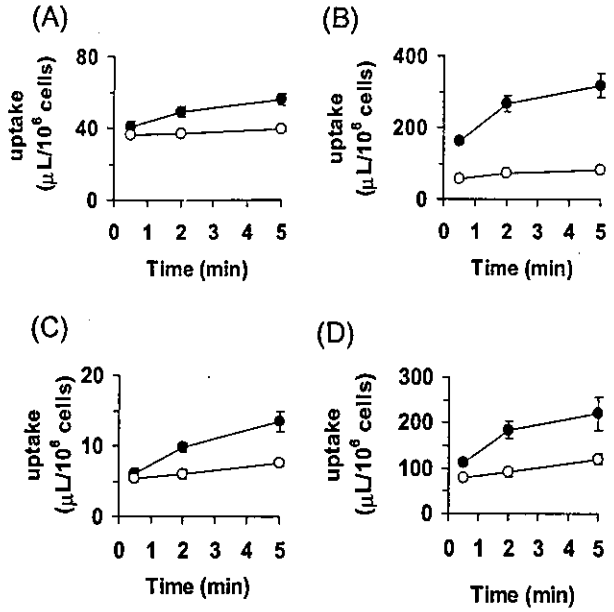

Fig. 2. Time profiles of the uptake of [^{3}H]E_2 17βG, [^{3}H]E-sul, [^{3}H]CCK-8, and [^{14}C]pitavastatin by human hepatocytes (Lot. ETR). The uptake of these substrates for 0.5, 2, and 5 min was determined at two concentrations (closed circle, 1 μM; open circle, 100 μM) at 37°C. Each point represents the mean ± S.E. (n = 3).

TABLE 2

Uptake clearance of reference compounds (E-sul and CCK-8) and test compounds (pitavastatin and $E_2$17βG) in human hepatocytes

Substrate	Uptake Clearance (CL_{hep})[a]		
	Lot. OCF	Lot. 094	Lot. ETR
	μl/min/10^6 cells		
E-sul	110	134	57.7
CCK-8	7.89	3.50	2.02
pitavastatin	61.3	113	39.2
$E_2$17βG	13.5	17.0	5.5

[a] Uptake clearance was determined using three independent batches of human cryopreserved hepatocytes.

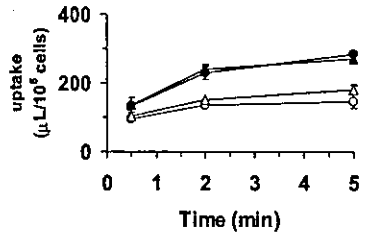

Fig. 3. Time profiles of the uptake of [^{14}C]pitavastatin by human hepatocytes (Lot. OCF) in the presence and absence of Na^+. The uptake of pitavastatin for 0.5, 2, and 5 min was determined at two concentrations (closed symbol, 1 μM; open symbol, 100 μM) at 37°C. Circles and triangles indicate the pitavastatin uptake in the presence and absence of Na^+, respectively. Each point represents the mean ± S.E. (n = 3).

regression line in Fig. 4, C and D reflected the relative expression level of each transporter in the transfectants and hepatocytes.

Estimation of Uptake Clearance and Contribution of OATP2 and OATP8 in Human Hepatocytes. We calculated the estimated uptake clearance of OATP2 and OATP8 in human hepatocytes by two approaches (Tables 3 and 4). In the first approach, by comparing the uptake clearance of reference compounds (E-sul for OATP2 and CCK-8 for OATP8) in transfectants and hepatocytes, we were able to

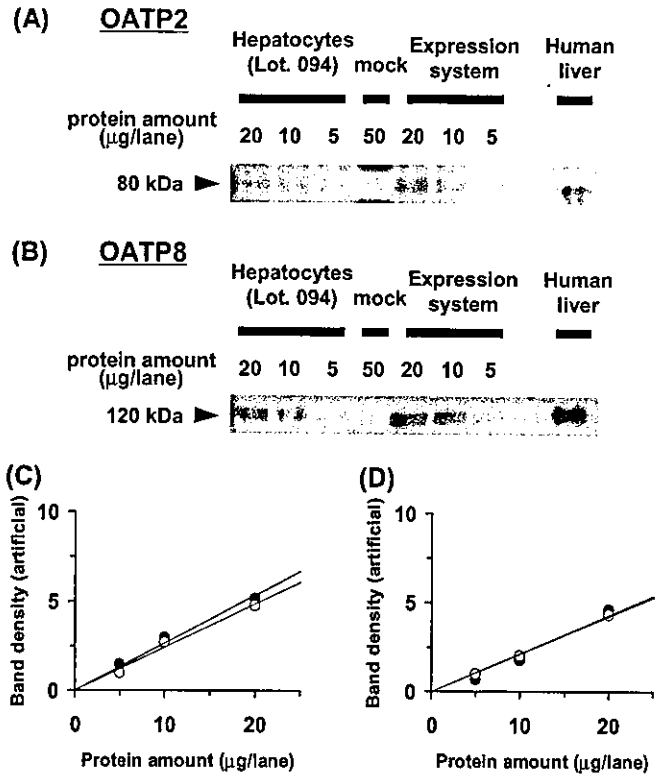

Fig. 4. Western blot analysis of OATP2 and OATP8. Crude membrane fractions (5, 10, and 20 μg) prepared from OATP2- and OATP8-expressed HEK293 cells and human hepatocytes (Lot. 094) were loaded and separated by SDS-PAGE (7% separating gel). The sample indicated "Human liver" means the crude membrane vesicles prepared from a human frozen liver block as a positive control. OATP2 and OATP8 were detected by preimmune antisera raised against the carboxyl terminus of human OATP2 (A) and OATP8 (B), respectively. Comparison of the relative expression levels of OATP2 (C) and OATP8 (D) between transfectants and hepatocytes is shown. The x-axis and y-axis represent the amount of crude membrane obtained from transfectants and human hepatocytes and the intensity of the specific band in Western blot analysis, respectively. Closed circles and open circles indicate the band density of human hepatocytes (Lot. 094) and OATP2- (C) or OATP8- (D) expressing HEK293 cells, respectively.

calculate the ratio of the clearance (R_{act}) and estimated clearance of pitavastatin and $E_2$17βG mediated by OATP2 and OATP8 based on the RAF method (Table 3). In the second approach, we compared the intensity of specific bands of transfectants and hepatocytes in Western blot analysis. We could obtain 62.1 and 96.7 μg of protein in crude membrane from 1 mg of whole cell protein in OATP2- and OATP8-expressing HEK293 cells, respectively, whereas 178, 89, and 82 μg of protein in crude membrane were obtained from 10^6 hepatocytes of Lot. OCF, 094, and ETR, respectively. When the band density per unit protein amount in crude membrane of OATP2- or OATP8-expressing HEK293 cells was defined as 1, the relative expression level of OATP2 or OATP8 per unit protein amount in crude membrane of hepatocytes of Lot. OCF, 094, and ETR was 1.01, 1.10, and 0.673 (per microgram) for OATP2 and 0.659, 1.01, and 0.872 (per microgram) for OATP8, respectively. Using these values, the relative ratio of the expression level (R_{exp}) and estimated clearance could be calculated (Table 4). The estimation by the two approaches suggested that both pitavastatin and $E_2$17βG are taken up into human hepatocytes predominantly by OATP2 (Tables 3 and 4).

TABLE 3
Contribution of OATP2 and OATP8 to the hepatic uptake of pitavastatin and $E_2$17βG determined using transporter-selective substrates

Hepatocyte Lot	Ratio of Uptake Clearance $CL_{hep}/CL_{transporter}$		Estimated Clearance[a]			
			Pitavastatin		$E_2$17βG	
	$R_{act,OATP2}$	$R_{act,OATP8}$	OATP2	OATP8	OATP2	OATP8
			$\mu l/min/10^6$ cells			
OCF	0.833	0.291	63.8	8.92	13.2	0.218
			87.7%	12.3%	98.4%	1.63%
094	1.02	0.131	77.8	4.01	16.0	0.0979
			95.1%	4.91%	99.4%	0.607%
ETR	0.437	0.0757	33.5	2.32	6.91	0.0565
			93.5%	6.47%	99.2%	0.812%

[a] The second line entry under "Estimated Clearance" shows the percentage of OATP2- or OATP8-mediated uptake clearance relative to the sum of the estimated clearance mediated by OATP2 and OATP8. The details of this estimation are described under *Materials and Methods*.

TABLE 4
Contribution of OATP2 and OATP8 to the hepatic uptake of pitavastatin and $E_2$17βG determined by the relative expression level

Hepatocyte Lot	Ratio of Expression Level[a] Hepatocyte Transporter		Estimated Clearance[b]					
			E-sul	CCK-8	Pitavastatin		$E_2$17βG	
	$R_{exp,OATP2}$	$R_{exp,OATP8}$	OATP2	OATP8	OATP2	OATP8	OATP2	OATP8
					$\mu l/min/10^6$ cells			
OCF	2.90	1.21	383	32.3	222	37.0	45.8	2.80
					85.7%	14.3%	94.2%	5.76%
094	1.58	0.930	208	24.8	121	28.4	24.9	2.15
					80.9%	19.1%	92.1%	7.95%
ETR	0.89	0.737	117	19.7	68.1	22.6	14.0	1.71
					75.1%	24.9%	89.2%	10.8%

[a] Ratio of the expression level was determined by the intensity of the specific band in the crude membrane prepared from human hepatocytes (per 10^6 cells) divided by that in the crude membrane from transporter-expressing cells (per milligram) in Western blot analysis.
[b] The second line entry under "Estimated Clearance" shows the percentage of the OATP2- or OATP8-mediated uptake clearance relative to the sum of the estimated clearance mediated by OATP2 and OATP8. The details of this estimation are described under *Materials and Methods*.

Discussion

In the present study, we have clarified that pitavastatin is taken up into human hepatocytes via OATP2 and OATP8, and we also investigated the transport properties of pitavastatin using transporter-expressing HEK293 cells and human cryopreserved hepatocytes to estimate the contribution of these transporters to the total uptake in human hepatocytes.

Significant uptake of pitavastatin via OATP2 and OATP8 was observed compared with control cells, and this became saturated on increasing its concentration in the medium (Fig. 1). It has been shown that, in a series of statins, pravastatin, cerivastatin, and rosuvastatin are substrates of OATP2 (Brown et al., 2001; Nakai et al., 2001; Sasaki et al., 2002; Shitara et al., 2003a). The K_m value of pitavastatin for OATP2 is comparable with that of cerivastatin (K_m = 4.3 μM) (in-house data) and rosuvastatin (K_m = 7.3 μM) (Brown et al., 2001) and smaller than that of pravastatin (K_m = 24.3 μM) (Sasaki et al., 2002).

We demonstrated here for the first time that, as far as statins are concerned, pitavastatin is a substrate for OATP8 as well as OATP2 (Fig. 1D). K_m values of pitavastatin for OATP2 and 8 were comparable (Fig. 1; Table 1); therefore, we were not able to determine which transporter is mainly responsible for its uptake in human hepatocytes only by saturation kinetics in human hepatocytes.

It has been reported that E-sul and CCK-8 are selective substrates of OATP2 and OATP8, respectively (Cui et al., 2001; Ismair et al., 2001). We confirmed these findings in our experimental systems (Fig. 1). We also confirmed that $E_2$17βG was a good substrate for both OATP2 and OATP8 by using transporter-expressing cells (Fig. 1) (König et al., 2000a, b). As shown in Table 1, the K_m values of $E_2$17βG, E-sul, and CCK-8 were comparable with the reported values (Ismair et al., 2001; Tamai et al., 2001).

Next, we performed the uptake study in human cryopreserved hepatocytes. Shitara et al. (2003b) reported that large interbatch differences in uptake activity were observed in human cryopreserved hepatocytes probably due to differences in the conditions of isolation of the hepatocytes and cryopreservation as well as the interindividual variability in the expression and function of transporters. So, we carried out a study using three batches of hepatocytes prepared from three independent donors. In all three batches examined in the present study, pitavastatin, $E_2$17βG, E-sul, and CCK-8 were taken up in a time-dependent and saturable manner (Fig. 2).

We examined the uptake of pitavastatin in the presence and absence of Na^+ to determine whether Na^+-dependent uptake of pitavastatin was observed in human hepatocytes. In this experiment, we confirmed that the batch (Lot. OCF) used in the present study exhibited Na^+-dependent uptake of taurocholate (data not shown) to the same extent as shown in the previous report (Shitara et al., 2003b). However, the uptake of pitavastatin by hepatocytes did not change regardless of the presence of Na^+, suggesting that pitavastatin is mainly taken up in a Na^+-independent way, suggesting that Na^+-taurocholate-cotransporting polypeptide is not mainly involved in hepatic uptake of pitavastatin. Previous reports demonstrated that both OATP2 and OATP8 can transport substrates in an Na^+-independent manner (König et al.,

2000a,b), and these Na^+-independent transporters are involved in hepatic uptake of pitavastatin.

To estimate the contribution of OATP2 and OATP8 to the hepatic uptake of pitavastatin, we developed a method using reference compounds that were selective substrates of OATP2 or OATP8. Crespi and Penman (1997) proposed the RAF method using the ratio of the metabolic activity in human liver microsomes divided by the activity in each isoform-specific cytochrome P450 reaction. Applying the RAF concept to transporter research, Hasegawa et al. (2003) calculated the contribution of Oat1 and Oat3 to the renal uptake in rats by comparing the uptake clearance of reference compounds (*p*-aminohippurate for Oat1 and benzylpenicillin for Oat3) in kidney slices and Oat1- and Oat3-transfected cells. According to this method, assuming that both for OATP2 and OATP8, the intrinsic clearance per unit molecule in human hepatocytes is the same as that in the expression system, the ratio of the transport activity of reference compounds in human hepatocytes to that in transporter-expressing cells (R_{act}) should correspond to the relative expression level of each transporter. Multiplying R_{act} by the uptake clearance of pitavastatin and $E_2 17\beta G$ in each transfectant, we can estimate the OATP2- and OATP8-mediated portion of the uptake of pitavastatin and $E_2 17\beta G$ in hepatocytes. From our estimation described above, the sum of the calculated OATP2- and OATP8-mediated uptake was almost identical to the experimentally observed uptake clearances in the cases of both pitavastatin and $E_2 17\beta G$ (Tables 2 and 3). Therefore, the uptake of pitavastatin and $E_2 17\beta G$ by human hepatocytes could be fully explained by OATP2 and OATP8, and more than 87% of their total hepatic uptake could be accounted for by OATP2 in all three independent batches of human cryopreserved hepatocytes (Tables 2 and 3).

To validate our estimation, we directly compared the expression level of OATP2 and OATP8 between transfectants and hepatocytes by Western blot analysis and calculated the ratio of the expression level in these cells (R_{exp}) as described above. As a result of our estimation using R_{exp} values, the sum of the predicted OATP2- and OATP8-mediated uptake of pitavastatin and $E_2 17\beta G$ was 5 to 10 times higher than their observed clearance in hepatocytes (Tables 2 and 4), a finding that is not consistent with our earlier estimation based on the relative uptake clearance of the reference compounds. There are two possibilities to account for this discrepancy. Firstly, the recovery of each transporter protein in samples for Western blot analysis in transfectants and hepatocytes may be different. Secondly, the total amount of protein in the whole-cell crude membrane, which we measured in the present study, may not indicate the expression level of a functional transporter on the cell surface. On the other hand, our results indicated that the ratio of the R_{exp} values for OATP2 and OATP8 was comparable with that of the R_{act} values and therefore, the estimated contribution of each transporter was almost the same when using the two calculation approaches. The contribution of OATP2 to the hepatic uptake of pitavastatin and $E_2 17\beta G$ estimated from the R_{exp} value also indicated more than 75 and 85% of the overall uptake in all three batches of hepatocytes, respectively, suggesting that the results obtained by the two approaches are consistent, and OATP2 appears to be mainly responsible for the hepatic uptake of pitavastatin and $E_2 17\beta G$ although both compounds are partly taken up by OATP8.

Alcorn et al. (2002) have reported that the mRNA level of OATP-B is almost the same as that of OATP2 in human liver. Strictly speaking, E-sul is not a selective substrate of OATP2 because some reports have indicated that it can be taken up by OATP-B and OATP8 (Kullak-Ublick et al., 2001; Kobayashi et al., 2003; Ismair et al., 2003), although we could not observe significant uptake of E-sul via OATP8 (Fig. 1), and Cui et al. (2001) reported that OATP8-expressing HEK293 cells did not significantly take up E-sul. However, we believe that E-sul can be used as a specific substrate of OATP2 in hepatocytes for the following reason. Previous reports have demonstrated that CCK-8 can be transported by OATP8, but not OATP-B and OATP2 (Ismair et al., 2001), and that $E_2 17\beta G$ can be a substrate of OATP2 and OATP8, but not OATP-B (Kullak-Ublick et al., 2001; Tamai et al., 2001). Taking these facts into consideration, we believe that the hepatic uptake of $E_2 17\beta G$ can be almost completely accounted for by OATP2 because the contribution of OATP8 to the overall hepatic uptake of $E_2 17\beta G$ was negligible in our estimation based on the uptake clearance of CCK-8 (Table 3). On the other hand, the uptake clearance of $E_2 17\beta G$ in human hepatocytes was almost comparable with the OATP2-mediated uptake clearance of $E_2 17\beta G$ estimated from the uptake clearance of E-sul in human hepatocytes and the OATP2 expression system. Therefore, we believe that E-sul is taken up into human hepatocytes mainly by OATP2.

In clinical situations, Shitara et al. (2003a) suggested that the drug-drug interaction between cerivastatin and cyclosporin A is mediated by OATP2. Nishizato et al. (2003) reported that OATP-C*15 polymorphism affects plasma concentration of pravastatin. Therefore, OATP2 may play a major role in the hepatic uptake of statins, and we should pay attention to functional change of OATP2 in pharmacokinetics of statins.

In conclusion, we have evaluated the contribution of OATP2 and OATP8 to the hepatic uptake of pitavastatin and $E_2 17\beta G$ by transporter-expressing HEK293 cells and human hepatocytes. When we estimated their contribution by two approaches using the uptake of transporter-selective substrates and the relative expression level measured by Western blot analysis, most of the total hepatic clearance of pitavastatin and $E_2 17\beta G$ could be accounted for by OATP2. These methods will be useful for rapidly identifying the separate contributions of OATP2 and OATP8 to the hepatic uptake.

References

Alcorn J, Lu X, Moscow JA, and McNamara PJ (2002) Transporter gene expression in lactating and nonlactating human mammary epithelial cells using real-time reverse transcription-polymerase chain reaction. *J Pharmacol Exp Ther* **303**:487–496.

Aoki T, Nishimura H, Nakagawa S, Kojima J, Suzuki H, Tamaki T, Wada Y, Yokoo N, Sato F, Kimata H, et al. (1997) Pharmacological profile of a novel synthetic inhibitor of 3-hydroxy-3-methylglutaryl-coenzyme A reductase. *Arzneimittelforschung* **47**:904–909.

Brown CDA, Windass A, Bleasby K, and Lauffart B (2001) Rosuvastatin is a high affinity substrate of hepatic organic anion transporter OATP-C. *Atheroscler Suppl* **2**:90.

Crespi CL and Penman BW (1997) Use of cDNA-expressed human cytochrome P450 enzymes to study potential drug-drug interactions. *Adv Pharmacol* **43**:171–188.

Cui Y, Konig J, Leier I, Buchholz U, and Keppler D (2001) Hepatic uptake of bilirubin and its conjugates by the human organic anion transporter SLC21A6. *J Biol Chem* **276**:9626–9630.

Davidson MH, Stein EA, Dujovne CA, Hunninghake DB, Weiss SR, Knopp RH, Illingworth DR, Mitchel YB, Melino MR, Zupkis RV, et al. (1997) The efficacy and six-week tolerability of simvastatin 80 and 160 mg/day. *Am J Cardiol* **79**:38–42.

Fujino H, Saito T, Tsunenari Y, and Kojima J (2003) Interaction between several medicines and statins. *Arzneimittelforschung* **53**:145–153.

Hagenbuch B and Meier PJ (1996) Sinusoidal (basolateral) bile salt uptake systems of hepatocytes. *Semin Liver Dis* **16**:129–136.

Hagenbuch B and Meier PJ (2003) The superfamily of organic anion transporting polypeptides. *Biochim Biophys Acta* **1609**:1–18.

Hasegawa M, Kusuhara H, Endou H, and Sugiyama Y (2003) Contribution of organic anion transporters to the renal uptake of anionic compounds and nucleoside derivatives in rat. *J Pharmacol Exp Ther* **305**:1087–1097.

Hsiang B, Zhu Y, Wang Z, Wu Y, Sasseville V, Yang WP, and Kirchgessner TG (1999) A novel human hepatic organic anion transporting polypeptide (OATP2): identification of a liver-specific human organic anion transporting polypeptide and identification of rat and human hydroxymethylglutaryl-CoA reductase inhibitor transporters. *J Biol Chem* **274**:37161–37168.

Ismair MG, Stanca C, Ha HR, Renner EL, Meier PJ, and Kullak-Ublick GA (2003) Interactions of glycyrrhizin with organic anion transporting polypeptides of rat and human liver. *Hepatol Res* **26**:343–347.

Ismair MG, Stieger B, Cattori V, Hagenbuch B, Fried M, Meier PJ, and Kullak-Ublick GA (2001) Hepatic uptake of cholecystokinin octapeptide by organic anion-transporting polypeptides OATP4 and OATP8 of rat and human liver. *Gastroenterology* **121**:1185–1190.

Kajinami K, Takekoshi N, and Saito Y (2003) Pitavastatin: efficacy and safety profiles of a novel synthetic HMG-CoA reductase inhibitor. *Cardiovasc Drug Rev* **21**:199–215.

Kimata H, Fujino H, Koide T, Yamada Y, Tsunenari Y, Yonemitsu M, and Yanagawa Y (1998) Studies on the metabolic fate of NK-104, a new inhibitor of HMG-CoA reductase: I. Absorption, distribution, metabolism and excretion in rats. *Xenobio Metabol Dispos* **13**:484–498.

Kobayashi D, Nozawa T, Imai K, Nezu J, Tsuji A, and Tamai I (2003) Involvement of human organic anion transporting polypeptide OATP-B (SLC21A9) in pH-dependent transport across intestinal apical membrane. *J Pharmacol Exp Ther* **306**:703–708.

Kojima J, Ohshima T, Yoneda M, and Sawada H (2001) Effect of biliary excretion on the pharmacokinetics of pitavastatin (NK-104) in dogs. *Xenobio Metab Disp* **16**: 497–502.

König J, Cui Y, Nies AT, and Keppler D (2000a) Localization and genomic organization of a new hepatocellular organic anion transporting polypeptide. *J Biol Chem* **275**:23161–23168.

König J, Cui Y, Nies AT, and Keppler D (2000b) A novel human organic anion transporting polypeptide localized to the basolateral hepatocyte membrane. *Am J Physiol Gastrointest Liver Physiol* **278**:G156–164.

Kullak-Ublick GA, Ismair MG, Stieger B, Landmann L, Huber R, Pizzagalli F, Fattinger K, Meier PJ, and Hagenbuch B (2001) Organic anion-transporting polypeptide B (OATP-B) and its functional comparison with three other OATPs of human liver. *Gastroenterology* **120**:525–533.

Kullak-Ublick GA, Stieger B, and Meier PJ (2004) Enterohepatic bile salt transporters in normal physiology and liver disease. *Gastroenterology* **126**:322–342.

Muller M and Jansen PL (1997) Molecular aspects of hepatobiliary transport. *Am J Physiol* **272**:G1285–1303.

Nakai D, Nakagomi R, Furuta Y, Tokui T, Abe T, Ikeda T, and Nishimura K (2001) Human liver-specific organic anion transporter, LST-1, mediates uptake of pravastatin by human hepatocytes. *J Pharmacol Exp Ther* **297**:861–867.

Nishizato Y, Ieiri I, Suzuki H, Kimura M, Kawabata K, Hirota T, Takane H, Irie S, Kusuhara H, Urasaki Y, et al. (2003) Polymorphisms of OATP-C (SLC21A6) and OAT3 (SLC22A8) genes: consequences for pravastatin pharmacokinetics. *Clin Pharmacol Ther* **73**:554–565.

Sasaki M, Suzuki H, Ito K, Abe T, and Sugiyama Y (2002) Transcellular transport of organic anions across a double-transfected Madin-Darby canine kidney II cell monolayer expressing both human organic anion-transporting polypeptide (OATP2/SLC21A6) and multidrug resistance-associated protein 2 (MRP2/ABCC2). *J Biol Chem* **277**:6497–6503.

Shimada S, Fujino H, Morikawa T, Moriyasu M, and Kojima J (2003) Uptake mechanism of pitavastatin, a new inhibitor of HMG-CoA reductase, in rat hepatocytes. *Drug Metab Pharmakokinet* **18**:245–251.

Shitara Y, Itoh T, Sato H, Li AP, and Sugiyama Y (2003a) Inhibition of transporter-mediated hepatic uptake as a mechanism for drug-drug interaction between cerivastatin and cyclosporin A. *J Pharmacol Exp Ther* **304**:610–616.

Shitara Y, Li AP, Kato Y, Chuang LU, Ito K, Itoh T, and Sugiyama Y (2003b) Function of uptake transporters for taurocholate and estradiol 17β-D-glucuronide in cryopreserved human hepatocytes. *Drug Metab Pharmakokinet* **18**:33–41.

Sugiyama D, Kusuhara H, Shitara Y, Abe T, Meier PJ, Sekine T, Endou H, Suzuki H, and Sugiyama Y (2001) Characterization of the efflux transport of 17beta-estradiol-D-glucuronide from the brain across the blood-brain barrier. *J Pharmacol Exp Ther* **298**:316–322.

Tamai I, Nozawa T, Koshida M, Nezu J, Sai Y, and Tsuji A (2001) Functional characterization of human organic anion transporting polypeptide B (OATP-B) in comparison with liver-specific OATP-C. *Pharm Res (NY)* **18**:1262–1269.

Yamaoka K, Tanigawara Y, Nakagawa T, and Uno T (1981) A pharmacokinetic analysis program (multi) for microcomputer. *J Pharmacobiodyn* **4**:879–885.

Address correspondence to: Dr. Yuichi Sugiyama, Department of Molecular Pharmacokinetics, Graduate School of Pharmaceutical Sciences, The University of Tokyo, 7-3-1 Hongo, Bunkyo-ku, Tokyo 113-0033, Japan. E-mail: sugiyama@mol.f.u-tokyo.ac.jp

0022-3565/04/3113-1147–1153$20.00
THE JOURNAL OF PHARMACOLOGY AND EXPERIMENTAL THERAPEUTICS

JPET 311:1147–1153, 2004

Vol. 311, No. 3
71621/1179070
Printed in U.S.A.

Involvement of Multiple Transporters in the Efflux of 3-Hydroxy-3-methylglutaryl-CoA Reductase Inhibitors across the Blood-Brain Barrier

Ryota Kikuchi, Hiroyuki Kusuhara, Takaaki Abe, Hitoshi Endou, and Yuichi Sugiyama

Department of Molecular Pharmacokinetics, Graduate School of Pharmaceutical Sciences, the University of Tokyo, Tokyo, Japan (R.K., H.K., Y.S.); Division of Nephrology, Endocrinology, and Vascular Medicine, Department of Medicine, Tohoku University Graduate School of Medicine, Sendai, Japan (T.A.); and Department of Pharmacology and Toxicology, Kyorin University School of Medicine, Tokyo, Japan (H.E.)

Received May 18, 2004; accepted August 3, 2004

ABSTRACT

Statins, 3-hydroxy-3-methylglutaryl-CoA reductase inhibitors, are frequently used for the treatment of hypercholesterolemia. The present study aimed to examine the involvement of organic anion transporters in the efflux transport of pravastatin and pitavastatin across the blood-brain barrier (BBB). Transport studies using cDNA-transfected cells revealed that these statins are substrates of multispecific organic anion transporters expressed at the BBB (rOat3:*Slc22a8* and rOatp2:*Slco1a4*). The efflux of these statins across the BBB was characterized using the brain efflux index method. The efflux clearance of pitavastatin across the BBB, obtained from the elimination rate constant and the distribution volume in the brain, was greater than that of pravastatin (364 versus 59 μl/min/g brain). The efflux of pravastatin and pitavastatin was saturable (apparent K_m values: 18 and 5 μM, respectively) and inhibited by probenecid but unaffected by tetraethylammonium. Furthermore, an inhibitor of the efflux pathway for hydrophilic organic anions across the BBB (*p*-aminohippurate), and inhibitors of the efflux pathway for amphipathic organic anions (taurocholate and digoxin) inhibited the efflux of both statins. The degree of inhibition by *p*-aminohippurate was similar and partial for the efflux of pravastatin and pitavastatin. Taurocholate and digoxin completely inhibited the efflux of pitavastatin, whereas their effect was partial for the efflux of pravastatin. The results of the present study suggest the involvement of multiple transporters, including rOat3 and rOatp2, in the efflux transport of pravastatin and pitavastatin across the BBB, each making a different contribution.

The brain capillary endothelial cells are characterized by highly developed tight junctions and the expression of xenobiotic transporters (Kusuhara and Sugiyama, 2001a,b; Lee et al., 2001; Golden and Pollack, 2003; Sun et al., 2003). These transporters include the member(s) of the Oat family (Oat3) (Ohtsuki et al., 2002; Kikuchi et al., 2003), the Oatp family (Oatp2) (Asaba et al., 2000; Sugiyama et al., 2001), and the ATP-binding cassette transporters (Mdr1 and Mrp1) (Kusuhara et al., 1997; Sugiyama et al., 2003). Cumulative evidence suggests that these transporters facilitate the elimination of xenobiotics and endogenous compounds from the central nervous system (CNS) across the BBB, providing the barrier function between the blood and the brain.

Statins, HMG-CoA reductase inhibitors, have been used for the treatment of hypercholesterolemia. HMG-CoA reductase, the rate-limiting enzyme in cholesterol biosynthesis, is present in the liver and nonhepatic tissues, catalyzing the early conversion of HMG-CoA to mevalonic acid, and the enzyme inhibition in the liver by statins results in the lower serum level of total cholesterol (Reinoso et al., 2002). The adverse effects of statins include CNS side effects, such as sleep disturbance, as well as myopathy (Schaefer, 1988; Barth et al., 1990). Therefore, the liver selectivity of statins must be given priority in clinical situations to reduce the undesired toxicological effects on the body. On the other hand, several reports suggest that statins have a potentially neuroprotective effect (Cucchiara and Kasner, 2001). Thus, it is possible that statins could be used for the treatment of CNS diseases. Previously, Saheki et al. (1994) showed that the brain uptake clearance of pravastatin was quite low, almost comparable with that of sucrose using the in situ brain perfusion technique. However, taking into consideration the chronic administration of statins, it is necessary to

This work was supported by grants-in-aid from the Ministry of Education, Culture, Sports, Science and Technology of Japan.
Article, publication date, and citation information can be found at http://jpet.aspetjournals.org.
doi:10.1124/jpet.104.071621.

ABBREVIATIONS: Oat, organic anion transporter; Oatp, organic anion-transporting polypeptide; CNS, central nervous system; BBB, blood-brain barrier; HMG, 3-hydroxy-3-methylglutaryl; BEI, brain efflux index; PAH, *p*-aminohippurate; TCA, taurocholate.

investigate the efflux transport across the BBB since the steady-state brain concentration is governed by both the uptake and the efflux transport across the BBB.

Pitavastatin, one of the newly developed statins, contains a carboxyl acid group in its chemical structure like pravastatin. Although pitavastatin is more lipophilic than pravastatin (log $D_{7.0}$: 1.5 versus −0.47) (Ishigami et al., 2001), its brain-to-plasma concentration ratio has been reported to be lower than that of pravastatin (0.063 versus 0.48) (Komai et al., 1992; Kimata et al., 1998). The lower distribution of pitavastatin in the brain may be explained by the efflux transport across the BBB.

We have recently shown that rOat3 is expressed at the BBB (Kikuchi et al., 2003). rOat3 is a multispecific transporter, with substrates that include amphipathic organic anions as well as hydrophilic ones (Kusuhara et al., 1999). According to inhibition studies, it has been suggested that rOat3 is involved in the efflux of hydrophilic organic anions, but its contribution to the efflux transport of amphipathic organic anions, such as 17β-estradiol-D-17β-glucuronide, is limited (Sugiyama et al., 2001; Kikuchi et al., 2003). rOatp2, another multispecific organic anion transporter expressed at the BBB (Gao et al., 1999), has been suggested to account for the efflux of amphipathic organic anions across the BBB (Asaba et al., 2000; Hosoya et al., 2000; Sugiyama et al., 2001). Since pravastatin is a substrate of both rOat3 and rOatp2 (Tokui et al., 1999; Hasegawa et al., 2002), these transporters may be involved in the efflux of pravastatin and, possibly, of pitavastatin, from the brain across the BBB, accounting for the lower brain distribution of pitavastatin compared with that of pravastatin.

In the present study, we demonstrated that pravastatin and pitavastatin are substrates of both rOat3 and rOatp2 using cDNA-transfected cells. The efflux clearances of pravastatin and pitavastatin from the brain into the blood circulation across the BBB were calculated using the intracerebral microinjection technique (BEI method) and brain slice uptake experiments. In addition, the involvement of rOat3 and rOatp2 in the efflux processes was suggested in vivo by examining the inhibitory effect of several compounds.

Materials and Methods

Chemicals. [^{3}H]Pravastatin (45.5 Ci/mmol) and unlabeled pravastatin sodium [(+)-(3*R*,5*R*)-3,5-dihydroxy-7-[(1*S*,2*S*,6*S*,8*S*,8a*R*)-6-hydroxy-2-methyl-8-[(*S*)-2-methylbutyryloxy]-1,2,6,7,8,8a-hexahydro-1-naphthyl]heptanoate] were kindly donated by Sankyo (Tokyo, Japan), and [^{3}H]pitavastatin (16 Ci/mmol) and unlabeled pitavastatin [(+)-monocalcium bis[(3*R*,5*S*,6*E*)-7-[2-cyclopropyl-4-(4-fluorophenyl)-3-quinolyl]-3,5-dihydroxy-6-heptenoate] were supplied by Kowa Company Ltd. (Tokyo, Japan). [^{14}C]Carboxyl-inulin (2.5 mCi/g) was purchased from PerkinElmer Life and Analytical Sciences (Boston, MA). Unlabeled probenecid, PAH, and TCA were purchased from Sigma-Aldrich (St. Louis, MO), unlabeled digoxin was obtained from Aldrich Chemical Co. (Milwaukee, WI), and unlabeled tetraethylammonium was purchased from Wako Pure Chemicals (Osaka, Japan). Ketamine hydrochloride was purchased from Sankyo. Xylazine and ketamine hydrochloride were used as anesthetics. All other chemicals were commercially available, of reagent grade, and used without further purification.

Animals. Sprague-Dawley male rats (supplied by Japan SLC, Shizuoka, Japan) weighing 220 to 250 g were used throughout this study and had free access to food and water. All experiments using animals in this study were carried out according to the guidelines provided by the Institutional Animal Care Committee (Graduate School of Pharmaceutical Sciences, The University of Tokyo).

Transport Study. rOat3- and rOatp2-expressed LLC-PK1 cells were established and maintained as described previously (Sugiyama et al., 2001). Uptake was initiated by adding the radiolabeled ligands to the medium in the presence and absence of inhibitors after cells had been washed three times and preincubated with Krebs-Henseleit buffer at 37°C for 15 min. The Krebs-Henseleit buffer consisted of 142 mM NaCl, 23.8 mM $NaHCO_3$, 4.83 mM KCl, 0.96 mM KH_2PO_4, 1.20 mM $MgSO_4$, 12.5 mM HEPES, 5 mM glucose, and 1.53 mM $CaCl_2$ adjusted to pH 7.4. The uptake was terminated at designated times by adding ice-cold Krebs-Henseleit buffer, dissolved in 500 μl of 0.2 N NaOH and kept overnight. The radioactivity associated with the cells and medium was determined. The aliquots of cell lysate were used to determine the protein concentration by the method of Lowry (1951), with bovine serum albumin as a standard. Ligand uptake is given as the cell-to-medium concentration ratio determined as the amount of ligand associated with the cells divided by the medium concentration.

In Vivo Efflux Study. The efflux of test compounds from the brain after microinjection into the cerebral cortex was investigated using the BEI method as described previously (Kakee et al., 1996). [^{3}H]Pravastatin (15.6 nCi/rat) or [^{3}H]pitavastatin (31.3 nCi/rat) with a nonpermeable reference compound [[^{14}C]carboxyl-inulin (0.625 nCi/rat)] in 0.5 μl of ECF buffer (122 mM NaCl, 25 mM $NaHCO_3$, 10 mM D-glucose, 3 mM KCl, 1.4 mM $CaCl_2$, 1.2 mM $MgSO_4$, 0.4 mM K_2HPO_4, and 10 mM HEPES, pH 7.4) in the presence or the absence of different concentrations of various inhibitors was injected into the Par2 region (0.2 mm anterior and 5.5 mm lateral to the bregma, 4.5 mm in depth). After the microinjection, rats were decapitated, and the radioactivity that remained in the left and right cerebrum was determined. The 100-BEI (%), which represents the remaining percentage of the test compounds in the cerebrum, is described by eq. 1.

$$100 - \mathrm{BEI}\ (\%) = \frac{\dfrac{\text{amount of test drug in the brain}}{\text{amount of reference in the brain}}}{\dfrac{\text{amount of test drug injected}}{\text{amount of reference injected}}} \times 100 \quad (1)$$

The elimination rate constant of the compounds from the brain (k_{el}) was obtained by fitting the 100-BEI (%) versus time data. A nonlinear least-squares regression program (MULTI) (Yamaoka et al., 1981) was used for the calculation.

Measurement of the Distribution Volume of [^{3}H]Pravastatin and [^{3}H]Pitavastatin in the Brain. The distribution volume of pravastatin and pitavastatin in the brain was determined by the in vitro brain slice uptake technique. Brain slices were prepared as reported previously with a minor modification (Kakee et al., 1997). A hypothalamic slice, 300-μm thick, was cut using a brain microslicer (DTK-2000; Dosaka, Kyoto, Japan), and kept in oxygenated ECF buffer equilibrated with 95% O_2/5% CO_2. After preincubation for 5 min at 37°C, the brain slice (15–25 mg) was transferred to 3 ml of oxygenated incubation medium containing [^{3}H]pravastatin or [^{3}H]pitavastatin (0.05 μCi/ml) and [^{14}C]carboxyl-inulin (0.01 μCi/ml) at 37°C. At appropriate times, brain slices were collected, and the radioactivity was determined in a liquid scintillation counter. Ligand uptake was given as the amount of ligand associated with the slice divided by the medium concentration.

Results

Time Profiles of the Uptake of [^{3}H]Pravastatin and [^{3}H]Pitavastatin by cDNA-Transfected Cells. The uptake of [^{3}H]pravastatin and [^{3}H]pitavastatin by rOat3- and rOatp2-transfected LLC-PK1 cells was significantly greater than that by vector-transfected cells (Fig. 1). The uptake of pravastatin by the cDNA-transfected cells increased linearly

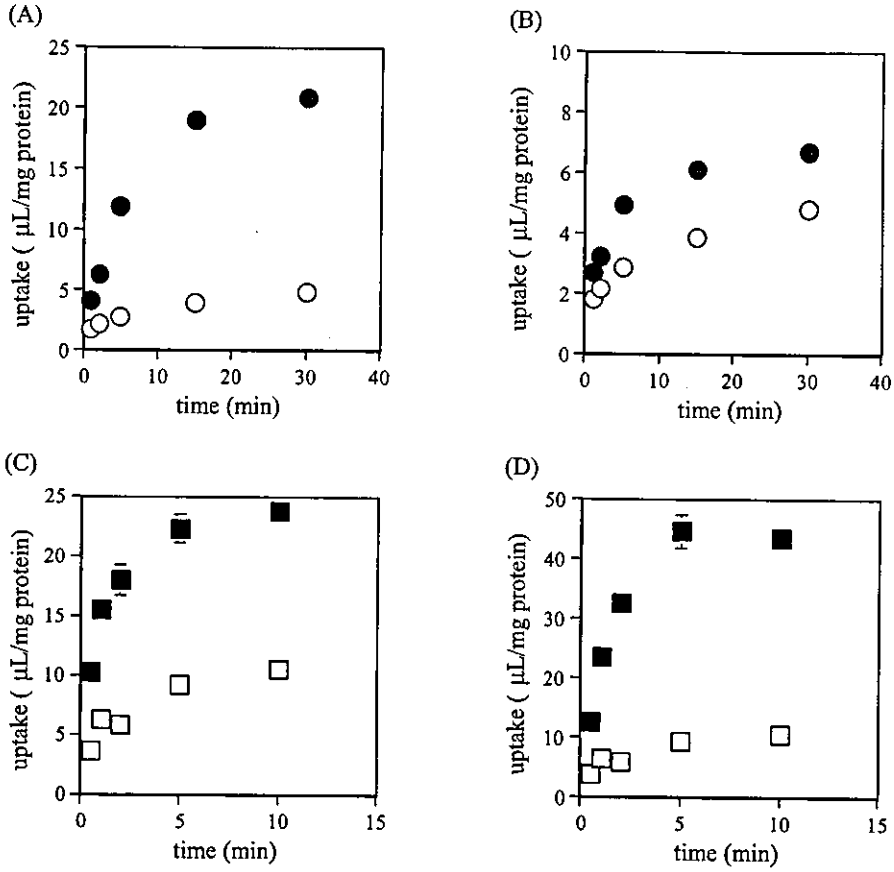

Fig. 1. Time profiles of the uptake of [^{3}H]pravastatin and [^{3}H]pitavastatin by gene-transfected LLC-PK1 cells. The uptake of [^{3}H]pravastatin (A and B) and [^{3}H]pitavastatin (C and D) by rOat3- (A and C) and rOatp2- (B and D) transfected LLC-PK1 cells was examined at 37°C. Circles and squares represent the uptake of [^{3}H]pravastatin and [^{3}H]pitavastatin, respectively. Closed and open symbols represent the uptake by gene- and vector-transfected cells, respectively. Each point represents the mean ± S.E. (n = 3).

over 5 min, whereas that of pitavastatin increased over 2 min. Eadie-Hofstee plots of the specific uptake of pitavastatin via rOat3 and rOatp2, obtained by subtracting the uptake by vector-transfected cells from that by cDNA-transfected cells, are shown in Fig. 2, A and B. Comparison of the Akaike's Information Criterion values (Yamaoka et al., 1981) suggested that the specific uptake of pitavastatin by rOat3 consists of one saturable component, and the K_m and V_{max} values of pitavastatin for rOat3 were determined as 0.982 ± 0.176 μM and 4.76 ± 0.53 pmol/min/mg protein, respectively (Fig. 2A). It was suggested that the specific uptake of pitavastatin by rOatp2 consists of one saturable and one nonsaturable component. The K_m and V_{max} values of pitavastatin for rOatp2 were 7.21 ± 0.96 μM and 80.9 ± 10.9 pmol/min/mg protein, respectively, and the uptake clearance corresponding to the nonsaturable component was 1.24 ± 0.25 μl/min/mg protein (Fig. 2B).

Time Profile of the Efflux of [^{3}H]Pravastatin and [^{3}H]Pitavastatin from the Brain across the BBB. The time profiles of the efflux of pravastatin and pitavastatin from the brain after microinjection into the cerebral cortex are shown in Fig. 3. Both statins were effluxed from the brain into the systemic circulation following microinjection, and k_{el} was calculated as 0.060 ± 0.002 min^{-1} for pravastatin and 0.026 ± 0.004 min^{-1} for pitavastatin.

Uptake of Pravastatin and Pitavastatin by Brain Slices. The distribution volume of pravastatin and pitavastatin in the brain, $V_{d,brain}$, was determined in the in vitro brain slice uptake study. Figure 4, A and B, shows the time profiles of the uptake of [^{3}H]pravastatin and [^{3}H]pitavasta-

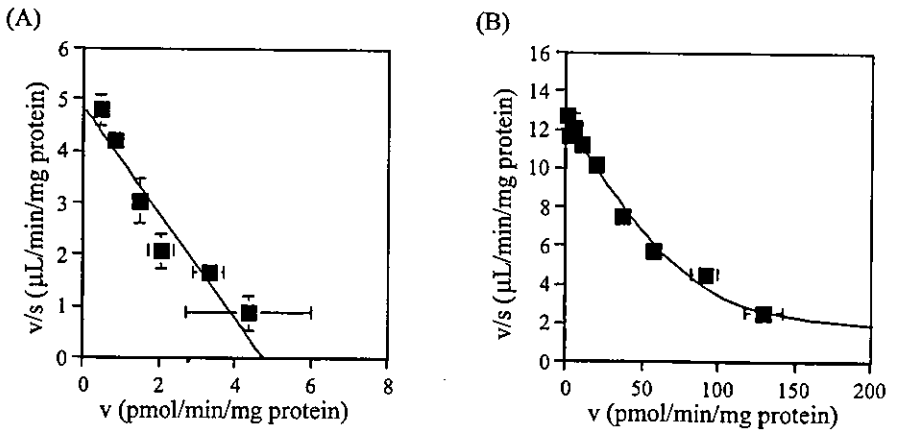

Fig. 2. Concentration dependence of the uptake of [^{3}H]pitavastatin by rOat3- and rOatp2-transfected LLC-PK1 cells. The uptake of [^{3}H]pitavastatin by rOat3- (A) and rOatp2- (B) transfected LLC-PK1 cells in the presence of unlabeled pitavastatin was examined at 37°C. Specific uptake was obtained by subtracting the uptake by vector-transfected cells from that by gene-transfected cells. The solid lines represent the fitted line obtained by nonlinear regression analysis. Each point represents the mean ± S.E. (n = 3).

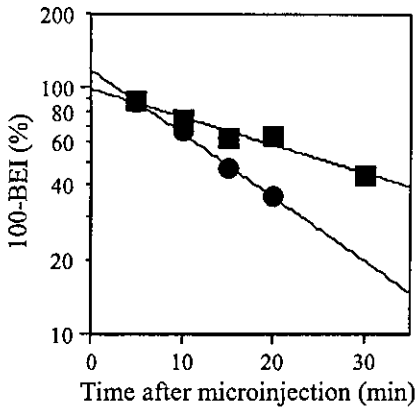

Fig. 3. Time profile of [^{3}H]pravastatin and [^{3}H]pitavastatin in the cerebrum after intracerebral microinjection. A mixture of [^{3}H]pravastatin (15.6 nCi/rat) or [^{3}H]pitavastatin (31.3 nCi/rat) and [^{14}C]carboxyl-inulin (0.625 nCi/rat) dissolved in 0.5 μl of ECF buffer was injected into Par2 of the rat cerebrum; subsequently, animals were decapitated at appropriate times. Circles and squares represent the elimination of pravastatin and pitavastatin, respectively. The solid line represents the fitted line obtained by nonlinear regression analysis. Each point represents the mean ± S.E. (n = 3).

tin by brain slices, respectively. For both statins, no significant differences in the slice-to-medium ratio between 120 and 240 min after incubation were observed, giving a steady-state slice-to-medium ratio ($V_{d,brain}$) of 0.989 ± 0.020 ml/g brain for pravastatin and 14.0 ± 0.4 ml/g brain for pitavastatin.

Calculation of the Efflux Clearances of Statins from the Brain into the Blood across the BBB. The apparent BBB efflux clearances (CL_{eff}) of pravastatin and pitavastatin were calculated by multiplying the apparent elimination rate constant (k_{el}) by the distribution volume in the brain ($V_{d,brain}$). The efflux clearances of pravastatin and pitavastatin were 59.3 ± 2.3 and 364 ± 57 μl/min/g brain, respectively.

Concentration-Dependent Efflux of Pravastatin and Pitavastatin from the Brain. The apparent elimination rate constant (k_{el}) of pravastatin and pitavastatin decreased while increasing the concentration of unlabeled substrate in the injectate (Fig. 5, A and B). Considering the dilution factor of 46.2 in the cerebrum after intracerebral microinjection (Kakee et al., 1996), the apparent Michaelis-Menten constant (K_m) for the efflux of pravastatin and pitavastatin from the brain across the BBB was estimated to be 18.2 ± 5.0 and 4.85 ± 1.14 μM, respectively.

Effect of Inhibitors on the Efflux of Statins across the BBB. The efflux of pravastatin and pitavastatin from the brain into the blood across the BBB was almost completely inhibited by 50 mM probenecid in the injectate whereas the effect of 50 mM tetraethylammonium was not significant for both statins (Fig. 6). The efflux of both statins was also inhibited by PAH, TCA, and digoxin in a concentration-dependent manner (Fig. 7).

Discussion

In the present study, the uptake of pravastatin and pitavastatin by rOat3- and rOatp2-transfected cells was determined, and the involvement of rOat3 and rOatp2 in the efflux transport across the BBB was examined.

Statins, except lovastatin and simvastatin which are administered in inactive lactone forms, are used in their active acid forms (Reinoso et al., 2002). Thus, it is possible that organic anion transporters are involved in regulating their brain concentrations. It has been shown that pravastatin is a substrate of both rOat3 and rOatp2 (Tokui et al., 1999; Hasegawa et al., 2002). Transport studies using cDNA-transfected cells demonstrated that pitavastatin is a substrate of both rOat3 and rOatp2 (Fig. 1). The transport activity of pravastatin and pitavastatin by rOat3 was comparable (Fig. 1, A and C), although the K_m value of pitavastatin (0.98 μM) was more than 10-fold smaller than that of pravastatin reported previously (13 μM) (Hasegawa et al., 2002). The transport activity of pitavastatin by rOatp2 was much greater than that of pravastatin (Fig. 1, B and D), and the K_m value of pitavastatin (7.2 μM) was approximately 5-fold smaller than that of pravastatin (38 μM) (Tokui et al., 1999). These results suggest the possibility that rOat3 and/or rOatp2 are involved in the efflux of statins from the brain across the BBB.

Pitavastatin was eliminated from the cerebral cortex more slowly than pravastatin after microinjection (Fig. 3). However, the intrinsic efflux clearance of pitavastatin from the brain across the BBB, calculated by multiplying the elimination rate constant by the distribution volume in the brain, was approximately 6-fold greater than that of pravastatin. The lower brain distribution of pitavastatin compared with that of pravastatin may be partly accounted for by the greater efflux clearance from the brain, although the difference in the uptake clearance from the blood circulation may

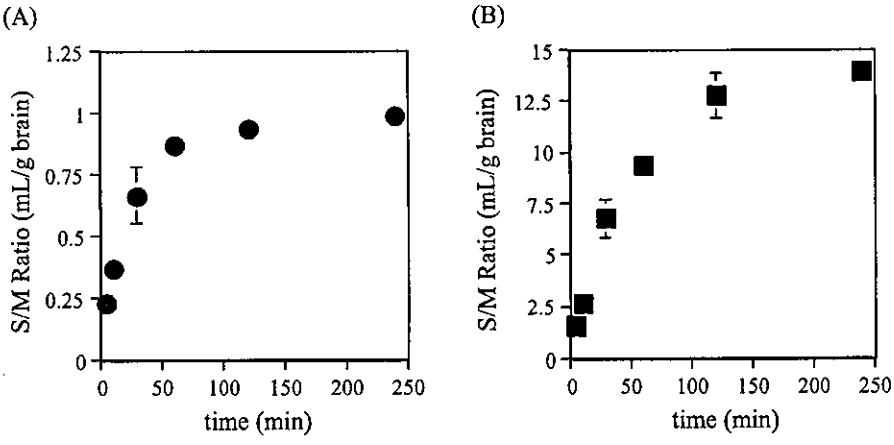

Fig. 4. Time courses of [^{3}H]pravastatin (A) and [^{3}H]pitavastatin (B) uptake by rat brain slices. Rat brain slices were incubated with 0.05 μCi/ml [^{3}H]pravastatin or [^{3}H]pitavastatin and 0.01 μCi/ml [^{14}C]carboxyl-inulin at 37°C. At appropriate times, the radioactivity in the brain slices and incubation medium was measured, and the slice-to-medium concentration ratio was estimated. Each point represents the mean ± S.E. (n = 3).

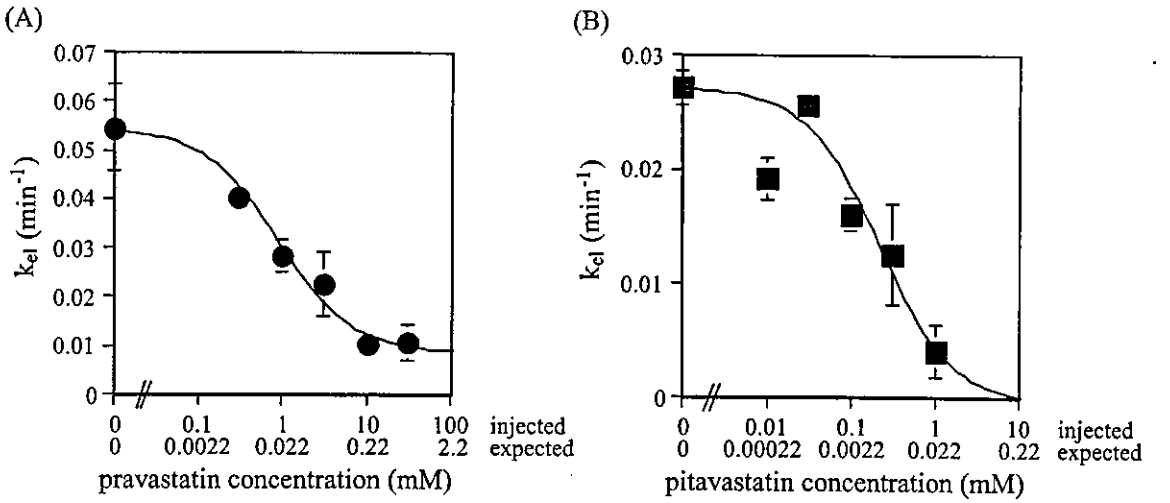

Fig. 5. Concentration dependence of the efflux of pravastatin and pitavastatin across the BBB. A, mixture of [^{3}H]pravastatin and [^{14}C]carboxyl-inulin dissolved in ECF buffer was injected into Par2 in the presence of 0, 0.3, 1, 3, 10, or 30 mM unlabeled pravastatin in the injectate. Rats were decapitated at 20 min after microinjection, and the elimination rate constant (k_{el}) was calculated. B, mixture of [^{3}H]pitavastatin and [^{14}C]carboxyl-inulin dissolved in saline was intracerebrally administered with 0, 0.01, 0.03, 0.1, 0.3, or 1 mM unlabeled pitavastatin in the injectate. Rats were decapitated at 30 min after microinjection, and the k_{el} value was calculated. Each value of the expected concentration was estimated by the concentration in the injectate divided by the dilution factor of 46.2 (Kakee et al., 1996). The solid lines represent the fitted line obtained by nonlinear regression analysis. Each point represents the mean ± S.E. (n = 3).

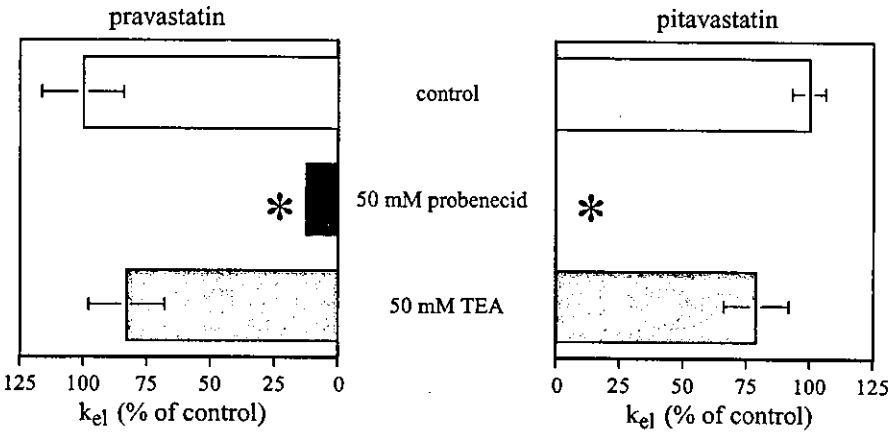

Fig. 6. Effect of unlabeled probenecid and tetraethylammonium on the efflux of [^{3}H]pravastatin (left column) or [^{3}H]pitavastatin (right column) from the cerebrum. ECF buffer containing [^{3}H]pravastatin or [^{3}H]pitavastatin and [^{14}C]carboxyl-inulin with or without unlabeled inhibitors was microinjected into Par2 of rat cerebrum, and the elimination rate constant (k_{el}) of [^{3}H]pravastatin or [^{3}H]pitavastatin was determined. The concentrations of inhibitors are shown as the injected concentration. Results are given as a ratio with respect to the elimination rate constant determined in the absence of inhibitors. Each column represents the mean ± S.E. (n = 3). *, significantly different from the control by Student's t test ($p < 0.05$).

also be one of the reasons. The efflux clearance of pravastatin was more than 3-fold greater than the previously reported uptake clearance (59 versus 18 μl/min/g brain) (Saheki et al., 1994). These results led us to conclude that there is asymmetrical transport of pravastatin across the BBB. The in vivo uptake clearance of pitavastatin into the brain may be low because of its high plasma protein binding. Thus, it is possible that the transport of pitavastatin across the BBB is also asymmetrical.

The involvement of transporters in the efflux of pravastatin and pitavastatin was investigated in vivo using the BEI method. The efflux transport of statins across the BBB was determined at different substrate concentrations. The efflux of the two statins was saturable with the saturable fraction accounting for the majority of their total efflux (Fig. 5). To obtain some insight into the transporters involved, inhibition studies were carried out. The efflux of pravastatin and pitavastatin from the brain was almost completely inhibited by the simultaneous injection of probenecid, but tetraethylammonium had no effect (Fig. 6). Furthermore, PAH (Kakee et al., 1997; Kikuchi et al., 2003) or TCA and digoxin (Kitazawa et al., 1998; Sugiyama et al., 2001) have been used as selective inhibitors for the efflux transport of hydrophilic or amphipathic organic anions across the BBB, respectively. The efflux of both statins was inhibited by these inhibitors in a concentration-dependent manner (Fig. 7). PAH inhibited the efflux of pravastatin and pitavastatin, but the inhibitory effect was partial (60% and 50%, respectively) even at the concentration sufficient to saturate its own efflux (Kakee et al., 1997; Kikuchi et al., 2003). TCA and digoxin inhibited the efflux of both statins; however, their maximum inhibitory effect differed significantly between pravastatin and pitavastatin (Fig. 7). They completely inhibited the efflux of pitavastatin, whereas their effect on the efflux of pravastatin was partial, suggesting the different contribution of the transporters involved. These results suggest that the efflux of

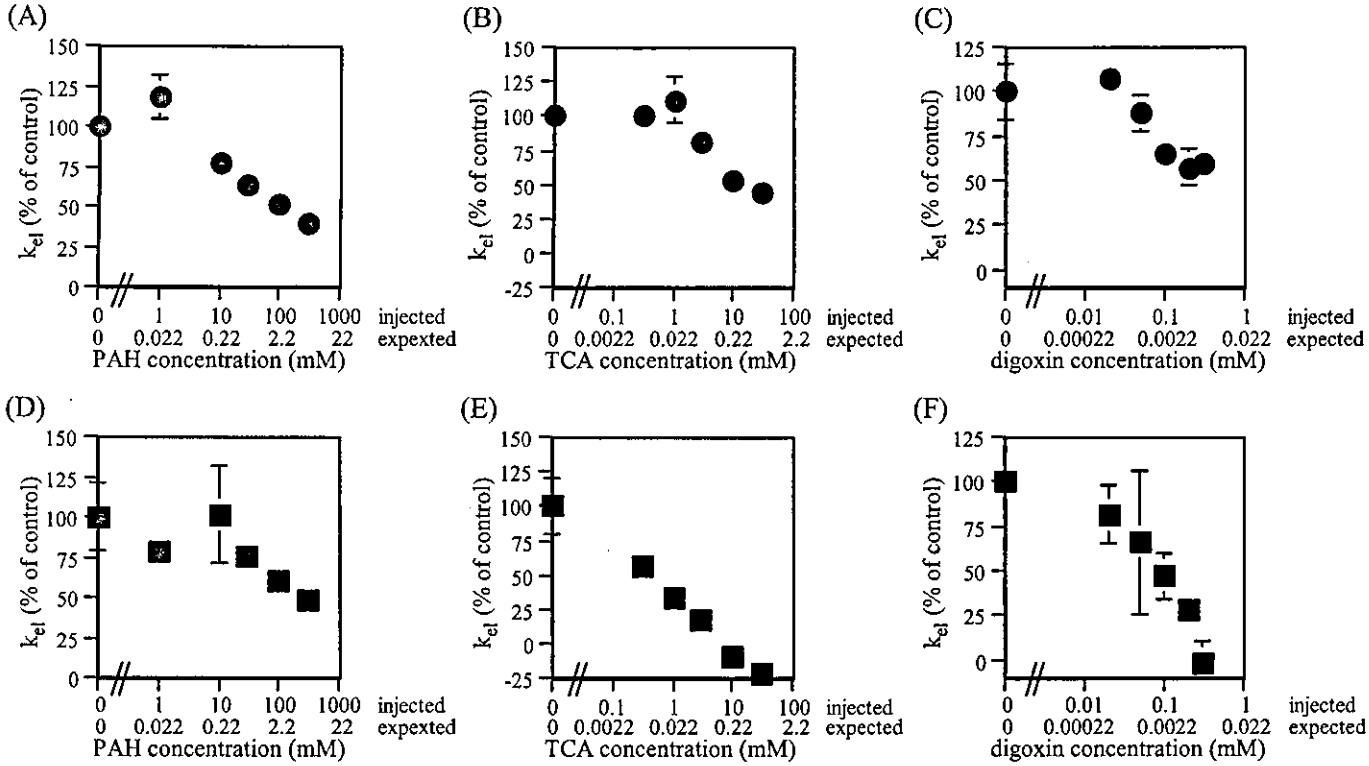

Fig. 7. Concentration dependence of the inhibitory effect of PAH, TCA, and digoxin on the efflux of [^{3}H]pravastatin or [^{3}H]pitavastatin from the cerebrum. ECF buffer containing [^{3}H]pravastatin (A–C) or [^{3}H]pitavastatin (D–F) and [^{14}C]carboxyl-inulin in the presence of different concentrations of PAH (A and D), TCA (B and E), and digoxin (C and F) was microinjected into Par2 of rat cerebrum, and k_{el} of [^{3}H]pravastatin or [^{3}H]pitavastatin was determined. Each value of the expected concentration was estimated considering the 46.2-fold dilution in the cerebrum after microinjection (Kakee et al., 1996). Results are given as a ratio with respect to the elimination rate constant determined in the absence of inhibitors. Each point represents the mean ± S.E. (n = 3).

statins consists of PAH-, TCA-, and digoxin-sensitive pathways. Since the efflux of 17β-estradiol-D-17β-glucuronide across the BBB after microinjection was completely inhibited by TCA, but partially by digoxin, the involvement of TCA-sensitive but digoxin-resistant transporters in the efflux of amphipathic organic anions has been suggested (Sugiyama et al., 2001). In the present study, TCA and digoxin inhibited the efflux of each statin to the same extent (Fig. 7). Therefore, it is likely that the TCA-sensitive but digoxin-resistant transporter(s) play a limited role in the efflux transport of statins across the BBB.

PAH has been used as an inhibitor of rOat3 (Kikuchi et al., 2003), whereas TCA has been used as an inhibitor of the amphipathic organic anion transport systems, including rOatp2, and digoxin is a specific inhibitor of rOatp2 (Sugiyama et al., 2001). The apparent K_m values of the efflux of pravastatin and pitavastatin were not very different from their K_m values for rOat3 and rOatp2: 13 and 38 μM for pravastatin (Tokui et al., 1999; Hasegawa et al., 2002), and 0.98 and 7.2 μM for pitavastatin (Fig. 2), respectively. The degree of inhibition of the efflux of pravastatin by PAH and TCA or digoxin was similar (Fig. 7, A–C) and accounted for the saturable fraction of the efflux transport. This result suggests the equal contribution of rOat3 and rOatp2 to the efflux transport of pravastatin across the BBB as high- and low-affinity sites, respectively. In the efflux transport of pitavastatin, the degree of inhibition by TCA or digoxin was greater than that by PAH (Fig. 7, D–F). However, the sum of the degree of inhibition by PAH and TCA or digoxin for the efflux of pitavastatin exceeded 100%. It is likely that these compounds inhibit other transporters at the BBB, including those expressed on the luminal membrane, since the net efflux across the BBB was evaluated by the BEI method. Assuming the PAH-sensitive fraction of the efflux of pravastatin represents the contribution of rOat3, the contribution of rOat3 to the efflux of pitavastatin across the BBB should be small since the transport activity of pitavastatin by rOat3 was similar to that of pravastatin (Fig. 1), and the intrinsic efflux clearance of pitavastatin was much greater than that of pravastatin. The difference between the transport activity of pravastatin and pitavastatin by rOatp2 may suggest a major contribution of rOatp2 to the efflux of pitavastatin across the BBB. Further studies are necessary to elucidate the transporters involved in the efflux of statins across the BBB.

Statins have been used for the drug treatment of hypercholesterolemia as inhibitors of HMG-CoA reductase. In addition to their lipid-lowering effects, increasing data suggest that these agents have properties that are potentially neuroprotective, i.e., endothelial protection via actions on the nitric oxide synthase system, as well as antioxidant, anti-inflammatory, and antiplatelet effects (Cucchiara and Kasner, 2001). Increasing the access of statins to the brain may improve their therapeutic effects in the CNS, although it may also increase the incidence of CNS side effects. The results of the present study indicate that increasing the lipophilicity is not necessarily followed by an improvement in the brain distribution, partly due to the difference in the efflux clearances from the brain. In vivo experiments such as in situ brain perfusion and the BEI method or in vitro ones using

BBB models, such as primary culture or immortalized cell lines and gene expression systems of the uptake and efflux transporters expressed at the BBB, will be required for the development of statins targeted to the CNS (Pardridge, 1998; Terasaki et al., 2003). Human OAT3 is expressed in the brain as shown by Northern blot analysis (Cha et al., 2001), and more recently, the expression of hOAT1 and hOAT3 at the choroid plexus, acting as a barrier between the blood and the cerebrospinal fluid, has been reported (Alebouyeh et al., 2003). Among the members of the human OATP family, hOATP-A has the highest homology to rOatp2 and is expressed at the BBB (Gao et al., 2000). It is possible that these human organic anion transporters play an important role in the efflux transport of organic anions across the barriers of the CNS. Their cDNA-transfected cells will provide screening systems for statins and other candidate drugs with anionic moieties.

In conclusion, both pravastatin and pitavastatin undergo efflux from the brain into the blood across the BBB, and at least two transporters, rOat3 and rOatp2, are involved in the efflux processes, each making a different contribution. It is likely that one of the underlying mechanisms of the lower brain distribution of pitavastatin compared with pravastatin despite its higher lipophilicity is the difference in the efflux transport clearance, i.e., in the transport activity by rOatp2.

Acknowledgments

We thank Sankyo (Tokyo, Japan) for providing labeled and unlabeled pravastatin and Kowa Company Ltd. (Tokyo, Japan) for providing labeled and unlabeled pitavastatin.

References

Alebouyeh M, Takeda M, Onozato ML, Tojo A, Noshiro R, Hasannejad H, Inatomi J, Narikawa S, Huang XL, Khamdang S, et al. (2003) Expression of human organic anion transporters in the choroid plexus and their interactions with neurotransmitter metabolites. *J Pharmacol Sci* **93**:430–436.

Asaba H, Hosoya K, Takanaga H, Ohtsuki S, Tamura E, Takizawa T, and Terasaki T (2000) Blood-brain barrier is involved in the efflux transport of a neuroactive steroid, dehydroepiandrosterone sulfate, via organic anion transporting polypeptide 2. *J Neurochem* **75**:1907–1916.

Barth JD, Kruisbrink OA, and Van Dijk AL (1990) Inhibitors of hydroxymethylglutaryl coenzyme A reductase for treating hypercholesterolaemia. *BMJ* **301**:669.

Cha SH, Sekine T, Fukushima JI, Kanai Y, Kobayashi Y, Goya T, and Endou H (2001) Identification and characterization of human organic anion transporter 3 expressing predominantly in the kidney. *Mol Pharmacol* **59**:1277–1286.

Cucchiara B and Kasner SE (2001) Use of statins in CNS disorders. *J Neurol Sci* **187**:81–89.

Gao B, Hagenbuch B, Kullak-Ublick GA, Benke D, Aguzzi A, and Meier PJ (2000) Organic anion-transporting polypeptides mediate transport of opioid peptides across blood-brain barrier. *J Pharmacol Exp Ther* **294**:73–79.

Gao B, Stieger B, Noe B, Fritschy JM, and Meier PJ (1999) Localization of the organic anion transporting polypeptide 2 (Oatp2) in capillary endothelium and choroid plexus epithelium of rat brain. *J Histochem Cytochem* **47**:1255–1264.

Golden PL and Pollack GM (2003) Blood-brain barrier efflux transport. *J Pharm Sci* **92**:1739–1753.

Hasegawa M, Kusuhara H, Sugiyama D, Ito K, Ueda S, Endou H, and Sugiyama Y (2002) Functional involvement of rat organic anion transporter 3 (rOat3; Slc22a8) in the renal uptake of organic anions. *J Pharmacol Exp Ther* **300**:746–753.

Hosoya K, Asaba H, and Terasaki T (2000) Brain-to-blood efflux transport of estrone-3-sulfate at the blood-brain barrier in rats. *Life Sci* **67**:2699–2711.

Ishigami M, Honda T, Takasaki W, Ikeda T, Komai T, Ito K, and Sugiyama Y (2001) A comparison of the effects of 3-hydroxy-3-methylglutaryl-coenzyme a (HMG-CoA) reductase inhibitors on the CYP3A4-dependent oxidation of mexazolam in vitro. *Drug Metab Dispos* **29**:282–288.

Kakee A, Terasaki T, and Sugiyama Y (1996) Brain efflux index as a novel method of analyzing efflux transport at the blood-brain barrier. *J Pharmacol Exp Ther* **277**:1550–1559.

Kakee A, Terasaki T, and Sugiyama Y (1997) Selective brain to blood efflux transport of para-aminohippuric acid across the blood-brain barrier: in vivo evidence by use of the brain efflux index method. *J Pharmacol Exp Ther* **283**:1018–1025.

Kikuchi R, Kusuhara H, Sugiyama D, and Sugiyama Y (2003) Contribution of organic anion transporter 3 (Slc22a8) to the elimination of *p*-aminohippuric acid and benzylpenicillin across the blood-brain barrier. *J Pharmacol Exp Ther* **306**: 51–58.

Kimata H, Fujino H, Koide T, Yamada Y, Tsunenari Y, and Yanagawa Y (1998) Studies on the metabolic fate of NK-104, a new inhibitor of HMG-CoA reductase: I. Absorption, distribution, metabolism and excretion in rats. *Xenobiol Metabol Dispos* **13**:484–498.

Kitazawa T, Terasaki T, Suzuki H, Kakee A, and Sugiyama Y (1998) Efflux of taurocholic acid across the blood-brain barrier: interaction with cyclic peptides. *J Pharmacol Exp Ther* **286**:890–895.

Komai T, Kawai K, Tokui T, Tokui Y, Kuroiwa C, Shigehara E, and Tanaka M (1992) Disposition and metabolism of pravastatin sodium in rats, dogs and monkeys. *Eur J Drug Metab Pharmacokinet* **17**:103–113.

Kusuhara H, Sekine T, Utsunomiya-Tate N, Tsuda M, Kojima R, Cha SH, Sugiyama Y, Kanai Y, and Endou H (1999) Molecular cloning and characterization of a new multispecific organic anion transporter from rat brain. *J Biol Chem* **274**:13675–13680.

Kusuhara H and Sugiyama Y (2001a) Efflux transport systems for drugs at the blood-brain barrier and blood-cerebrospinal fluid barrier (part 1). *Drug Discov Today* **6**:150–156.

Kusuhara H and Sugiyama Y (2001b) Efflux transport systems for drugs at the blood-brain barrier and blood-cerebrospinal fluid barrier (part 2). *Drug Discov Today* **6**:206–212.

Kusuhara H, Suzuki H, Terasaki T, Kakee A, Lemaire M, and Sugiyama Y (1997) P-Glycoprotein mediates the efflux of quinidine across the blood-brain barrier. *J Pharmacol Exp Ther* **283**:574–580.

Lee G, Dallas S, Hong M, and Bendayan R (2001) Drug transporters in the central nervous system: brain barriers and brain parenchyma considerations. *Pharmacol Rev* **53**:569–596.

Lowry O (1951) Protein measurement with the Folin phenol reagent. *J Biol Chem* **193**:265–273.

Ohtsuki S, Asaba H, Takanaga H, Deguchi T, Hosoya K, Otagiri M, and Terasaki T (2002) Role of blood-brain barrier organic anion transporter 3 (OAT3) in the efflux of indoxyl sulfate, a uremic toxin: its involvement in neurotransmitter metabolite clearance from the brain. *J Neurochem* **83**:57–66.

Pardridge WM (1998) CNS drug design based on principles of blood-brain barrier transport. *J Neurochem* **70**:1781–1792.

Reinoso RF, Sanchez Navarro A, Garcia MJ, and Prous JR (2002) Preclinical pharmacokinetics of statins. *Methods Find Exp Clin Pharmacol* **24**:593–613.

Saheki A, Terasaki T, Tamai I, and Tsuji A (1994) In vivo and in vitro blood-brain barrier transport of 3-hydroxy-3-methylglutaryl coenzyme A (HMG-CoA) reductase inhibitors. *Pharm Res (NY)* **11**:305–311.

Schaefer EJ (1988) HMG-CoA reductase inhibitors for hypercholesterolemia. *N Engl J Med* **319**:1222–1223.

Sugiyama D, Kusuhara H, Lee YJ, and Sugiyama Y (2003) Involvement of multidrug resistance associated protein 1 (Mrp1) in the efflux transport of 17beta estradiol-D-17beta-glucuronide (E217betaG) across the blood-brain barrier. *Pharm Res (NY)* **20**:1394–1400.

Sugiyama D, Kusuhara H, Shitara Y, Abe T, Meier PJ, Sekine T, Endou H, Suzuki H, and Sugiyama Y (2001) Characterization of the efflux transport of 17beta-estradiol-D-17beta- glucuronide from the brain across the blood-brain barrier. *J Pharmacol Exp Ther* **298**:316–322.

Sun H, Dai H, Shaik N, and Elmquist WF (2003) Drug efflux transporters in the CNS. *Adv Drug Deliv Rev* **55**:83–105.

Terasaki T, Ohtsuki S, Hori S, Takanaga H, Nakashima E, and Hosoya K (2003) New approaches to in vitro models of blood-brain barrier drug transport. *Drug Discov Today* **8**:944–954.

Tokui T, Nakai D, Nakagomi R, Yawo H, Abe T, and Sugiyama Y (1999) Pravastatin, an HMG-CoA reductase inhibitor, is transported by rat organic anion transporting polypeptide, oatp2. *Pharm Res (NY)* **16**:904–908.

Yamaoka K, Tanigawara Y, Nakagawa T, and Uno T (1981) A pharmacokinetic analysis program (multi) for microcomputer. *J Pharmacobiodyn* **4**:879–885.

Address correspondence to: Yuichi Sugiyama, Department of Molecular Pharmacokinetics, Graduate School of Pharmaceutical Sciences, The University of Tokyo, 7-3-1 Hongo, Bunkyo-ku, Tokyo 113-0033, Japan. E-mail: sugiyama@mol.f.u-tokyo.ac.jp

5 Oct 2004 :1308 AR AR232-PA45-28.tex XMLPublish[SM](2004/02/24) P1: JRX
AR REVIEWS IN ADVANCE10.1146/annurev.pharmtox.44.101802.121444
(Some corrections may occur before final publication online and in print)

Annu. Rev. Pharmacol. Toxicol. 2005. 45:689–723
doi: 10.1146/annurev.pharmtox.44.101802.121444

First published online as a Review in Advance on October 12, 2004

EVALUATION OF DRUG-DRUG INTERACTION IN THE HEPATOBILIARY AND RENAL TRANSPORT OF DRUGS

Yoshihisa Shitara,[1] Hitoshi Sato,[1] and Yuichi Sugiyama[2]
[1]*School of Pharmaceutical Sciences, Showa University, Shinagawa-ku, Tokyo 142-8555, Japan; email: shitara@pharm.showa-u.ac.jp, satohito@pharm.showa-u.ac.jp*
[2]*Graduate School of Pharmaceutical Sciences, University of Tokyo, Bunkyo-ku, Tokyo 113-0033, Japan; email: sugiyama@mol.f.u-tokyo.ac.jp*

Key Words transporter, pharmacokinetics, quantitative prediction of drug-drug interaction

■ **Abstract** Recent studies have revealed the import role played by transporters in the renal and hepatobiliary excretion of many drugs. These transporters exhibit a broad substrate specificity with a degree of overlap, suggesting the possibility of transporter-mediated drug-drug interactions with other substrates. This review is an overview of the roles of transporters and the possibility of transporter-mediated drug-drug interactions. Among the large number of transporters, we compare the K_i values of inhibitors for organic anion transporting polypeptides (OATPs) and organic anion transporters (OATs) and their therapeutic unbound concentrations. Among them, cephalosporins and probenecid have the potential to produce clinically relevant OAT-mediated drug-drug interactions, whereas cyclosporin A and rifampicin may trigger OATP-mediated ones. These drugs have been reported to cause drug-drug interactions in vivo with OATs or OATPs substrates, suggesting the possibility of transporter-mediated drug-drug interactions. To avoid adverse consequences of such transporter-mediated drug-drug interactions, we need to be more aware of the role played by drug transporters as well as those caused by drug metabolizing enzymes.

INTRODUCTION

The kidney and the liver play important roles in the elimination of drugs and xenobiotics from the body (1–5). Cumulative in vivo and in vitro studies have revealed the importance of transporters in the renal and hepatobiliary excretion of many drugs and other xenobiotics (1–5). Recent studies to investigate the molecular mechanism of renal and hepatobiliary excretion have revealed that multiple transporters are expressed in the kidney and liver in animals and humans, as well as revealing their function, tissue distribution, and intracellular localization (6–15). These transporters exhibit broad substrate specificity with a degree of overlap.

0362-1642/05/0210-0689$14.00